Electronic Supplementary Material (ESI) for Chemical Communications.

A 25 mA/cm^2 Dye-Sensitized Solar Cell Based on a Near-Infrared-Absorbing Organic Dye and Application of the Device in SSM-DSCs

*Hammad Cheema[a], Jonathon Watson[a], Adithya Peddapuram[a§], and Jared H. Delcamp[a]**

[a]*481 Coulter Hall, Department of Chemistry and Biochemistry, University of Mississippi, University, MS, 38677, USA.*

[§] *Present Address: VolvoChem, Richmond, California 94806, USA.*

*Hammad Cheema, hammad.a.cheema@gmail.com

*Jared H. Delcamp, delcamp@olemiss.edu

TABLE OF CONTENTS

1. General Procedures

All commercially obtained reagents were used as received. Thin-layer chromatography (TLC) was conducted with Sorbtech silica XHL TLC plates and visualized with UV lamp. Flash column chromatography was performed with Silicycle ultrapure silica gels P60, 40-63 μm (230-400 mesh) NMR spectra were recorded on a Bruker AMX 400, a Bruker Avance-500 (500 MHz) or a Bruker Avance-300 (300 MHz) spectrometer and reported in ppm using a solvent as an internal standard ($CDCl_3$ at 7.26 ppm). Peaks are reported as: (s = singlet, d = doublet, t = triplet, q = quartet, p = pentet/quintet, m = multiplet, br s = broad singlet; coupling constant (Hz); integration). Absorbance spectra were measured with a Cary 5000 UV−Vis−NIR spectrophotometer. Cyclic voltammetry curves were measured with a CH Instruments electrochemical analyzer. Measurements were taken using platinum wire counter electrode, Ag/AgCl reference electrode with ferrocene as an internal standard, and a glassy carbon working electrode. The electrolytic solvent used was 0.1 M Bu_4NPF_6 in CH_2Cl_2 (DCM). Ferrocene was used as a reference standard, taken as 0.7 V vs normal hydrogen electrode (NHE) in DCM. ATR-FTIR of samples were recorded on a Bruker Alpha FTIR spectrometer. D35 and Y123 were purchased from Dyenamo, Sweden, and used as it is. N719 and Black Dye were purchased from Solaronix, Switzerland and used as it is. $Co(bpy)_3^{3+/2+}$ was prepared by following the literature procedure.[1] 1H,1H,2H,2H-perfluorooctyltrimethoxysilane (PFTS) was purchased from Beantown Chemical Company. Chenodeoxycholic acid (CDCA) was purchased from Chem-Impex International. TEC 10, TEC15 and TEC7 were all purchased from Hartford Glass Company, Indiana, USA. Amorphous fluoropolymer Cytop (CTL-809) and CT-Sol.180 were purchased from Asahi Glass Company, Japan.

2. Synthetic Procedures

Briefly, 4-bromo-6-formylthieno[3,4-*b*]thiophene-2-carboxylic ester (**1**) was coupled to stannylated CPDT^{EtHx} (**2**) via a Stille coupling to give the linked π-bridge 3,4-TT-CPDT^{EtHx} (**3**) in 71% yield. *N*-bromosuccinimide (NBS) bromination of the CPDT π-bridge, and coupling to bis(hexyloxy)triphenyl amine boronic ester (**5**) gave the TAA-3,4-TT-CPDT^{EtHx} aldehyde in intermediate (**6**) in 44% yield over two steps. Finally, the synthesis of **AP25** was completed after Knoevenagel condensation to afford the target dye in 40% yield.

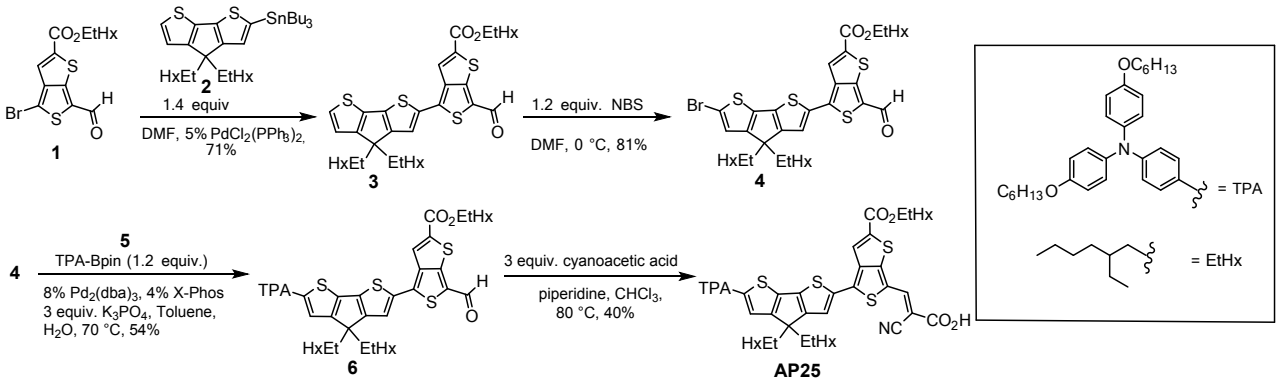

Scheme S1. Synthetic route to **AP25**.

2-ethylhexyl 4-(4,4-bis(2-ethylhexyl)-4H-cyclopenta[2,1-*b*:3,4-*b'*]dithiophen-2-yl)-6-formylthieno[3,4-*b*]thiophene-2-carboxylate (3):

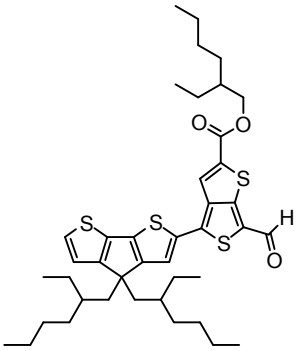

To a flame dried flask were added **1** (0.75 g, 1.87 mmol)[2], (4,4-bis(2-ethylhexyl)-4H-cyclopenta [2,1-b:3,4-b']dithiophen-2-yl)tributylstannane (**2**) (1.40 equiv., 1.80 g, 2.60 mmol)[3] and 19.0 mL of dry *N,N*-dimethylformamide (0.10 M). The mixture was purged with N_2 for 20 minutes, then $Pd(PPh_3)_2Cl_2$ (5.0 mol%, 66 mg, 94.1 μmol) was added and stirred under N_2 for 30 minutes at 70˚C. The reaction mixture was quenched with 15 mL of water, extracted (2 times) with 25 mL diethyl ether and then the organic layer was separated and dried with Na_2SO_4. After removal of solvent under reduced pressure, the crude mixture was subjected to silica gel column for purification with 10% ethylacetate/hexane as eluent, and dark orange solid was isolated (0.96 g, 71% yield). ^{1}H NMR (300 MHz, $CDCl_3$) δ 9.84 (s, 1H), 8.09 (s, 1H), 7.39 (s, 1H), 7.30 (d, *J* = 4.9 Hz, 1H), 7.00 (m, 1H), 4.29 (d, *J* = 5.6 Hz, 2H), 2.00-1.75 (m, 4H), 1.80-1.50 (m, 7H), 1.50-1.10 (m, 10H), 0.99-0.82 (m, 19H), 0.77-0.56 (m, 9H) ppm. ^{13}C NMR (75 MHz, $CDCl_3$) δ 179.0, 162.9, 160.1, 160.1, 159.3, 141.9, 141.7, 140.7, 140.7, 136.3, 133.9, 127.7, 123.5, 122.9, 122.8, 122.6, 68.7, 66.2, 54.3, 43.5, 39.2, 35.6, 34.6, 30.8, 29.3, 28.9, 28.3, 27.7, 27.2, 24.2, 23.3, 23.1, 20.0, 19.9, 17.8, 15.6, 14.4, 13.9, 11.4, 11.1, 11.0 ppm (Note: Due to alkane chain stereochemistry, multiple

diastereomers are present). IR (neat, cm^{-1}) 2956, 2924, 2861, 1715, 1642, 1527 cm^{-1}. HRMS ESI (positive mode) *m/z* calc'd for $C_{41}H_{56}O_3S_4Cs$ $[M + Cs]^+$: 857.2167, found 857.2177.

2-ethylhexyl 4-(6-bromo-4,4-bis(2-ethylhexyl)-4H-cyclopenta[2,1-*b*:3,4-*b*′]dithiophen-2-yl)-6-formylthieno[3,4-*b*]thiophene-2-carboxylate (4):

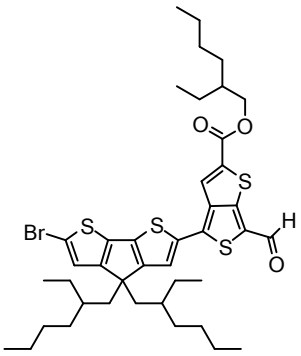

To a flame dried flask was added intermediate **3 (**1.0 g, 1.38 mmol) and *N,N*-dimethylformamide (17 mL, 0.10 M). The solution was allowed to stir at 0 ˚C for 10 minutes then *N*-bromosuccinamide (1.2 equiv., 0.294 g, 1.66 mmol) was added to the reaction flask at 0°C and allowed to stir at room temperature. After 2 hours, the reaction mixture was poured into water (10 mL) and the mixture was extracted with diethyl ether (30 mL) two times. The organic phase was washed with water (20 mL), dried with Na_2SO_4, and the solvent was removed under reduced pressure. The crude product was purified by a silica gel plug with ethyl acetate, affording a red solid (0.89 g, 81% yield). ^{1}H NMR (300 MHz, $CDCl_3$) δ 9.85 (s, 1H), 8.07 (s, 1H), 7.37 (m, 1H), 7.02 (ap t, *J* = 2.9 Hz, 1H), 4.29 (ap d, *J* = 5.1 Hz, 2H), 1.99-1.81 (m, 4H), 1.80-1.67 (m, 1H), 1.53-1.25 (m, 6H), 1.12-0.84 (m, 23H), 0.81 (t, *J* = 6.5 Hz, 6H), 0.74-0.58 (m, 9H) ppm. ^{13}C NMR (75 MHz, $CDCl_3$) δ 179.0, 162.8, 158.7, 158.5, 158.4, 158.4, 140.9, 136.6, 134.4, 126.0, 125.9, 123.4, 122.9, 122.7, 122.6, 114.0, 68.7, 55.1, 43.4, 39.2, 35.6, 35.6, 34.5, 34.5, 34.5, 30.8, 29.3, 28.9, 28.9, 28.9, 27.8, 24.3, 23.3, 23.1, 14.4, 14.4, 14.4, 11.4, 11.0, 11.0 ppm. (Note: Due to alkane chain stereochemistry, multiple diastereomers are present). IR (neat, cm^{-1}) 3074, 2955, 2919, 2854, 1709, 1638, 1534 cm^{-1}. HRMS ESI (positive mode) *m/z* calc'd for $C_{41}H_{55}BrO_3S_4Cs$ $[M + Cs]^+$: 935.1272, found 935.1260.

2-ethylhexyl 4-(6-(4-(bis(4-(hexyloxy)phenyl)amino)phenyl)-4,4-bis(2-ethylhexyl)-4H-cyclopenta[2,1-*b*:3,4-*b*′]dithiophen-2-yl)-6-formylthieno[3,4-*b*]thiophene-2-carboxylate (6):

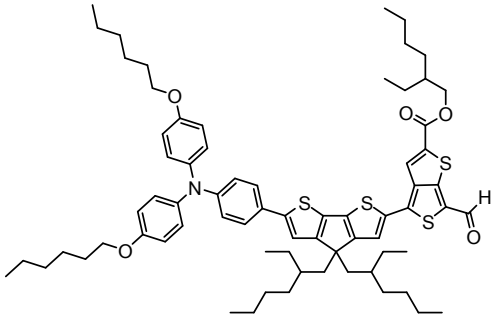

To a flame dried flask were added 2-ethylhexyl 4-(6-bromo-4,4-bis(2-ethylhexyl)-4H cyclopenta[2,1-*b*:3,4-*b*′]dithiophen-2-yl)-6 formylthieno[3,4-*b*]thiophene-2-carboxylate (**4**) (0.13 g, 0.16 mmol), TPA-Bpin (**5**) (1.2 equiv., 0.11 g, 0.194 mmol), toluene (6.4 mL, 0.025 M) and H_2O (0.29 mL, 0.55 M). The resulting mixture was purged with N_2 for 20 minutes, then Pd_2dba_3 (8.0 mol%, 11.0 mg, 129 μmol, X-Phos (4.0 mol%, 3.0 mg, 64 μmol) and K_3PO_4 (3.0 equiv., 103 mg, 0.486 mmol) were added in one portion. The reaction was stirred at 80 ˚C for 16 hours. The reaction mixture was quenched with 10 mL of water, extracted (2 times) with 20 mL diethyl ether and then the organic layer was separated and dried with Na_2SO_4. After removal of solvent under reduced pressure, the crude mixture was subjected to silica gel column for purification with 5% ethyl acetate/hexane as eluent, and purple solid was isolated (0.110 g, 54% yield). ^{1}H NMR (300 MHz,

$CDCl_3$) δ 9.83 (s, 1H), 8.10 (s, 1H), 7.45-7.35 (m, 3H), 7.08 (ap d, *J* = 8.4 Hz, 5H), 6.92 (d, *J* = 8.4 Hz, 2H), 6.84 (d, *J* = 8.8 Hz, 4H), 4.29 (ap d, *J* = 5.6 Hz, 2H), 3.94 (t, *J* = 6.5 Hz, 4H), 2.04-1.86 (m, 4H), 1.85-1.68 (m, 5H) 1.54-1.15 (m, 29H), 1.10-0.83 (m, 21H), 0.80-0.58 (m, 12H) ppm. ^{13}C NMR (75 MHz, $CDCl_3$) δ 178.8, 162.9, 161.3, 158.5, 156.1, 148.9, 148.3, 148.2, 142.6, 142.0, 140.6, 140.4, 134.2, 133.5, 127.1, 126.9, 126.5, 123.6, 122.8, 122.2, 120.5, 117.4, 117.3, 115.7, 68.7, 68.6, 54.6, 43.6, 39.2, 35.7, 35.6, 34.7, 34.5, 32.0, 30.8, 30.7, 30.0, 30.0, 29.7, 29.3, 29.0, 28.9, 27.7, 26.1, 24.3, 23.3, 23.1, 23.0, 14.4, 14.4, 14.4, 11.4, 11.1, 11.0, 11.0 ppm. (Note: Due to alkane chain stereochemistry, multiple diastereomers are present). IR (neat, cm^{-1}) 2926, 2861, 1714, 1640, 1602, 1504. HRMS ESI (positive mode) *m/z* calc'd for $C_{71}H_{93}NO_5S_4Cs$ $[M + Cs]^+$: 1300.4991, found 1300.5010.

(*E*)-3-(4-(6-(4-(bis(4-(hexyloxy)phenyl)amino)phenyl)-4,4-bis(2-ethylhexyl)-4H-cyclopenta[2,1-*b*:3,4-*b*′]dithiophen-2-yl)-2-(((2-ethylhexyl)oxy)carbonyl)thieno[3,4-*b*]thiophen-6-yl)-2-cyanoacrylic acid (AP25):

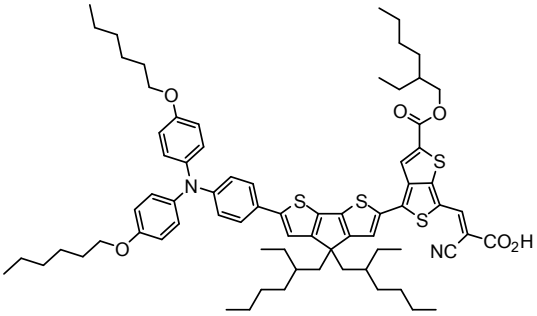

6 (98 mg, 79.0 μmol) was dissolved in $CHCl_3$ (7.8 mL, 0.01 M), cyanoacetic acid (20.0 mg, 0.23 mmol) and piperidine (46.0 mg, 0.54 mmol) under N_2. The reaction was heated to 80° C in a sealed vial and stirred for 5 hours. The reaction was acidified using AcOH (5 mL) diluted with diethyl ether (30 mL). Excess AcOH was removed by washing with H_2O (30 mL) three times. After removal of solvent under reduced pressure, the crude mixture was subjected to silica gel column for purification with 5% methanol/dichloromethane as eluent, and purple solid was isolated (40 mg, 40% yield). ^1H NMR (300 MHz, $CDCl_3$) δ 8.35 (s, 1H), 8.10 (s, 1H), 7.49 (s, 1H), 7.40 (d, *J* = 7.4 Hz, 2H), 7.08 (ap d, *J* = 8.5 Hz, 5H), 6.92 (d, *J* = 7.8 Hz, 2H), 6.84 (d, *J* = 8.8 Hz, 4H), 4.29 (d, *J* = 5.5 Hz, 2H), 3.94 (t, *J* = 6.5 Hz, 4H), 1.96 (ap br s, 4H), 1.83-1.74 (m, 5H), 1.50-1.15 (m, 29H), 1.10-0.80 (m, 21H), 0.80-0.60 (m, 12H) ppm. IR (neat, cm^{-1}) 2953, 2919, 2853, 1709, 1599, 1565, 1502. HRMS ESI (negative mode) *m/z* calc'd for $C_{74}H_{94}N_2O_6S_4Cs$ $[M + Cs]^+$: 1233.5917, found 1233.5938.

4. Sensitizer Optical and Electrochemical Data

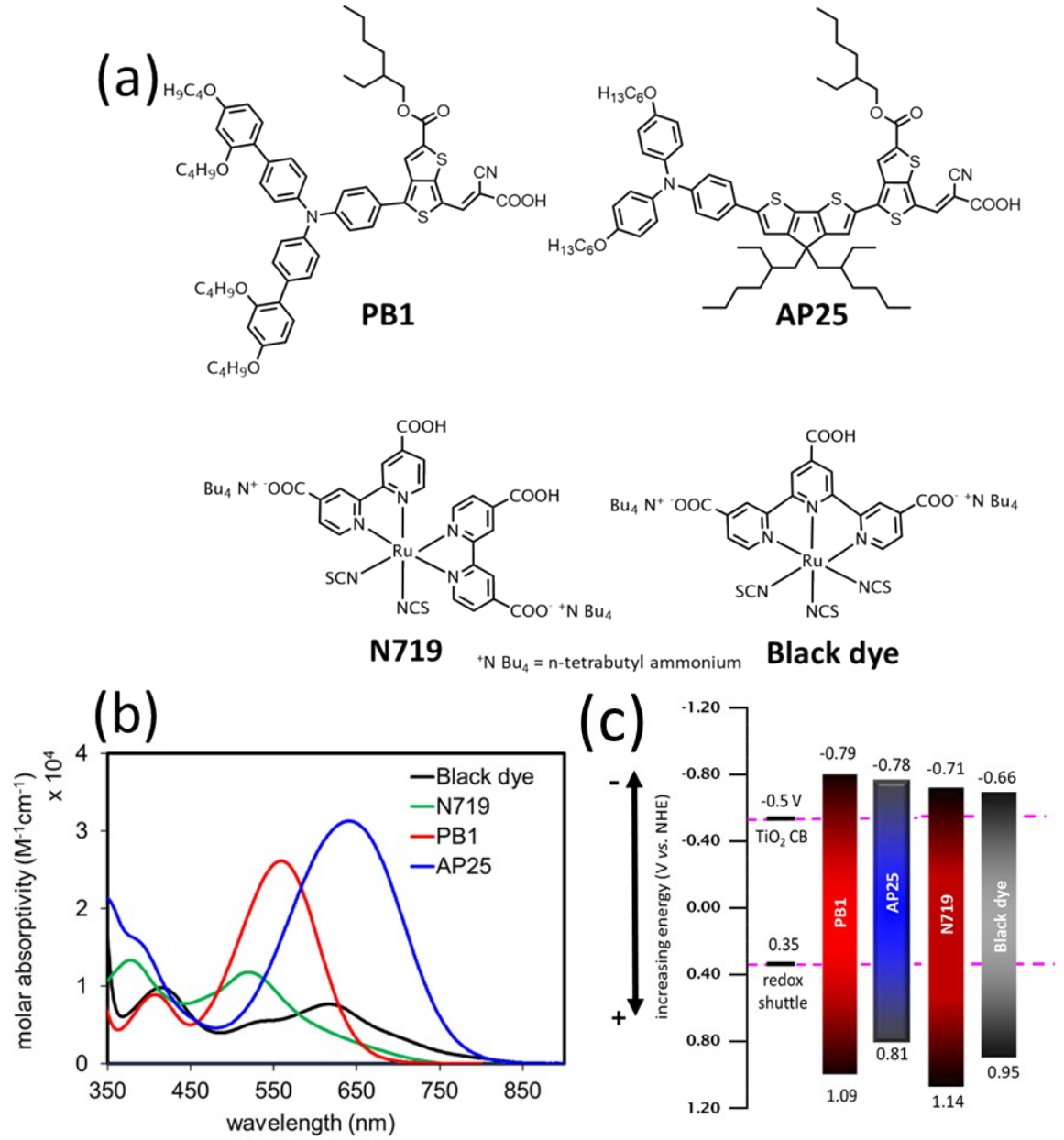

Figure S1. Comparing the **PB1**, **AP25, N719** and the **Black Dye** a) chemical structures, b) UV-Vis absorptions, and c) energetics.[2,4]

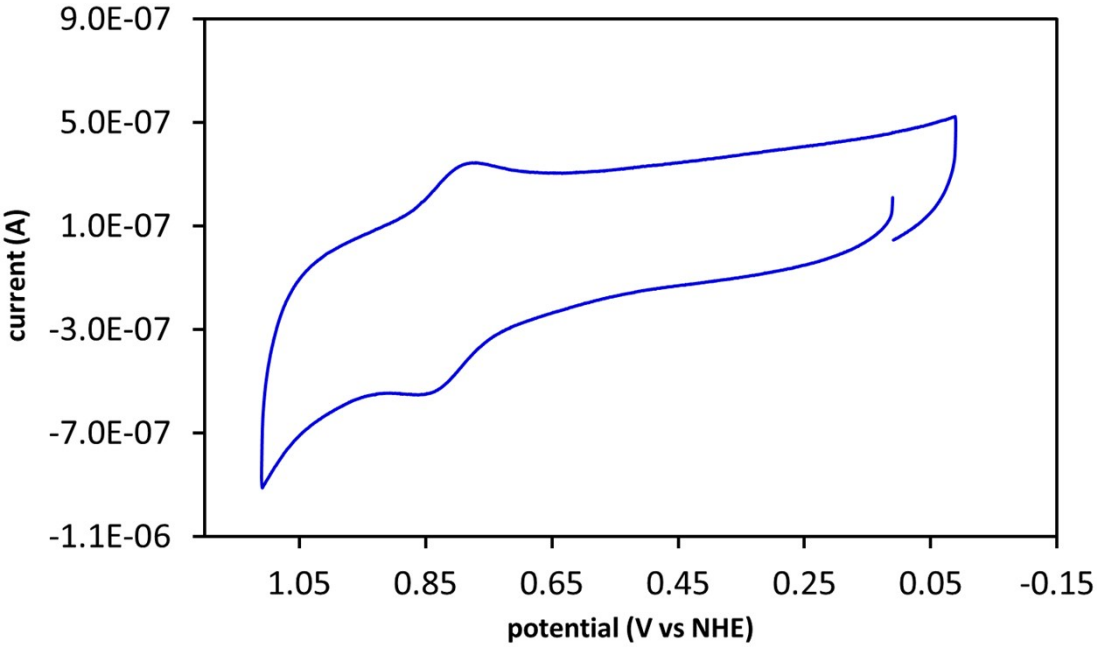

Figure S2. Cyclic voltammogram of **AP25** in DCM with a scan rate of 100 mV/s in a 0.1 M tetrabutylammonium hexafluorophosphate solution. A glassy carbon working electrode, platinum counter electrode, and silver wire reference were used. Ferrocene was used as an internal reference (not shown).

Table S1. Comparison of optical and electrochemical data for **PB1** and **AP25.**

Dye	λ_{max} [a] (nm)	λ_{onset} [b] (nm)	ε [a] ($M^{-1}cm^{-1}$)	$E_{(S+/S)}$ [c] (V)	$E_{(S+/S^*)}$ [d] (V)	E_g^{opt} [e] (eV)
PB1 [f]	560	665	26,000	1.09	-0.79	1.88
AP25	660	780	30,000	0.81	-0.78	1.59
N719 [f]	527	720	11740	1.14	-0.71	1.85
Black dye [f]	610	780	7640	0.95	-0.66	1.61

[a]Measured in CH_2Cl_2. [b]Onset values taken from the x-intercept of the downward tangent line of the absorbance curve on the low energy side. [c]Measured with a 0.1 M Bu_4NPF in CH_2Cl_2 solution using a glassy carbon working electrode, platinum reference electrode, and platinum counter electrode with ferrocene as an internal standard. Values are reported versus NHE. [d] $E_{(S+/S^*)}$ was calculated from the equation $E_{(S+/S^*)} = E_{(S+/S)} - E_g^{opt}$. [e]Estimated from the onset of the absorption curve in CH_2Cl_2. Conversion from nanometers to eV was calculated by $E_g^{opt} = 1240/\lambda_{onset}$. [f] PB1, N719 and Black Dye data was taken from previous reports.[2,4]

3. Computational Analysis: General Information

MM2 energy minimization in ChemBio3D Ultra (version:13.0.2.3021) was used for the initial energy minimization of **AP25**. Dihedral angles for the relevant groups were set to values between the global minimum and the next local minimum on the conformational energy diagram as calculated by chemBio3D. Accurate geometry optimization were performed sequentially by density functional theory (DFT) using Guassian09[5] with the B3LYP functional with the following basis sets: first 3-21g and second 6-311G(d,p) with default convergence thresholds and numerical integration grids. Time-dependent density functional theory (TD-DFT) computations were performed with optimized geometries and with the B3LYP functional and 6-311G(d,p) basis set to compute the vertical transition energies and oscillator strengths. All alkyl chains were truncated to simple methyl groups. Frequency calculations reveal no imaginary frequencies.

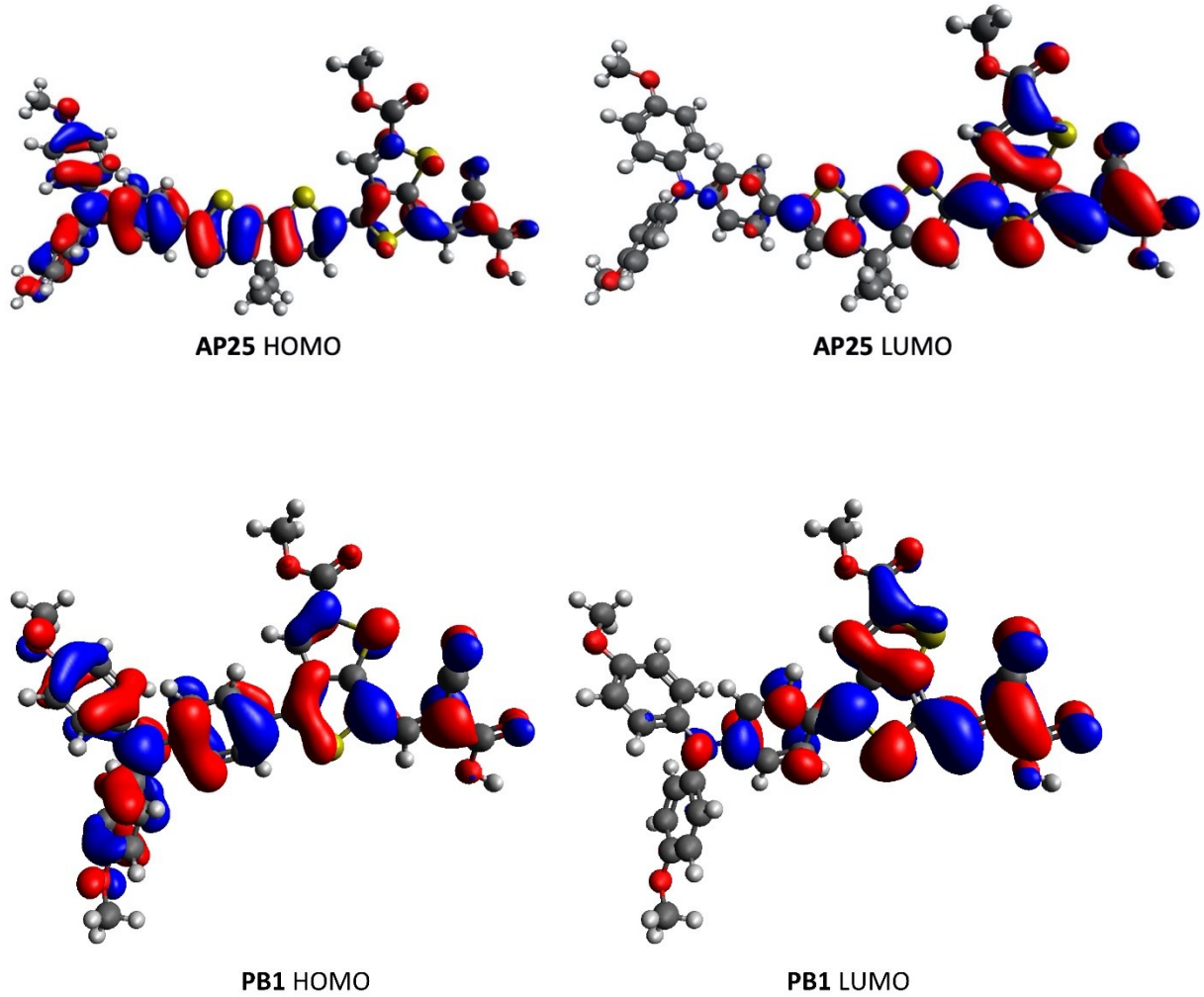

Figure S3. Frontier orbital distribution of **AP25** and **PB1** at the B3LYP/6-311G(d,p) level of theory. Iso values set to 0.02. XYZ coordinates are provided at end of the SI.

Table S2. Computational data from TD-DFT calculations.

Dye	State	Orbitals	contribution	vertical transition (eV | nm)	oscillator strength	exp. λ_{max} (eV | nm)	exp. ε ($M^{-1}cm^{-1}$)
AP25	S1	H → L	99%	1.86 | 666	1.1873	1.88 | 660	30000
AP25	S2	H-1 → L H → L+1	94% 4%	2.38 | 521	0.6051		
PB1	S1	H → L	99%	2.33 | 532	0.8665	2.21 | 560	26000
PB1	S2	H-1 → L H → L+1	51% 46%	2.93 | 423	0.0740		

"H" = HOMO; "L" = LUMO; "H-1" is the HOMO-1; "L+1" is the LUMO+1; S1 is excited state 1; S2 is excited state 2. S2 is provided to show that the next lowest energy excited state to the HOMO to LUMO transition is significantly lower in energy and not likely contributing to the charge transfer band seen in the absorption spectrum.

5. Device Measurement and Assembly Procedures

5.1. Photovoltaic Characterization

Photovoltaic characteristics were measured using a 150 W xenon lamp (Model SF300A, SCIENCETECH Inc. Class AAA) solar simulator equipped with an AM 1.5 G filter for a less than 2% spectral mismatch. Prior to each measurement, the solar simulator output was calibrated with a KG5 filtered mono-crystalline silicon NREL calibrated reference cell from ABET Technologies (Model 15150-KG5). The current density-voltage characteristic of each cell was obtained with Keithley digital source meter (Model 2400). The incident photon-to-current conversion efficiency was measured with an IPCE instrument manufactured by Dyenamo comprised of a 175 W xenon lamp (CERMAX, Model LX175F), monochromator (Spectral Products, Model CM110, Czerny-Turner, dual-grating), filter wheel (Spectral Products, Model AB301T, fitted with filter AB3044 [440 nm high pass] and filter AB3051 [510 nm high pass]), a calibrated UV-enhanced silicon photodiode reference and Dyenamo issued software.

5.2. Device Fabrication

For the photoanode, TEC 10 glass was cut into 2x2 cm squares, the substrate was submerged in a 0.2% Deconex 21 aqueous solution and sonicated for 15 minutes at room temperature. The electrodes were rinsed with water and sonicated in acetone for 10 minutes followed by sonication in ethanol for 10 minutes. Finally, the electrodes were placed under UV/ozone for 15 minutes (UV-Ozone Cleaning System, Model ProCleaner by UVFAB Systems). A compact TiO_2 underlayer is then applied by pretreatment of the substrate submerged in a 40 mM $TiCl_4$ solution in water (prepared from 99.9% $TiCl_4$ between 0-5 °C). The submerged substrates (conductive side up) were heated for 30 minutes at 70 °C. After heating, the substrates were first cooled down in the same solution to room temperature and then rinsed with water and ethanol. The photoanode consists of thin TiO_2 films comprising a 10-15 μm mesoporous TiO_2 layer (particle size, 20 nm, Dyesol, DSL 18NR-T) and a 5 μm TiO_2 scattering layer (particle size, 100 nm, Solaronix R/SP), respectively. Both layers were screen printed from a Sefar screen (54/137–64W) resulting in 5 μm thickness for each print. Between each print, the substrate was heated for 7 minutes at 125 ^oC and the thickness was measured with a profilometer (Alpha-Step D-500 KLA Tencor). The substrate was then sintered with progressive heating from 125 ^oC (5 minute ramp from r.t., 5-minute hold) to 325 ^oC (15 minute ramp from 125 ^oC, 5 minute hold) to 375 ^oC (5 minute ramp from 325 ^oC, 5 minute hold) to 450 ^oC (5 minute ramp from 375 ^oC, 15 minute hold) to 500 ^oC (5 minute ramp from 450 ^oC, 15 minute hold) using a programmable furnace (Vulcan® 3-Series Model 3-550). The cooled sintered photoanode was soaked 30 minutes at 70 ^oC in a 40 mM $TiCl_4$ water solution and heated again at 500 ^oC for 30 minutes prior to sensitization. The complete working electrode was prepared by immersing the TiO_2 film into the dye solution for overnight (~20 hours). The solution is 0.2 mM of **AP25** dye in ACN:*tert*-butanol with different amounts of CDCA. For **AP25**

single dye solution, 40x CDCA (8 mM) was optimal in ACN:*tert*-butanol with 0.2 mM concentration of the dye. For co-sensitized devices, 0.3 mM total dye concentration with **AP25:D35** (2:1) and the optimized amount of CDCA was 40x:10x i.e. (9 mM) in ACN:*tert*-butanol was employed.

Counter Electrode Preparation: Two holes were drilled through the taped FTO side of 2 x 2 cm squares of TEC 7 FTO glass (7 Ω/sq. sheet resistance) for full cells, and TEC 15 FTO glass (15 Ω/sq. sheet resistance) for all other subcells, using a Dremel-4000 with a Dremel 7134 Diamond Taper Point Bit submerged in water to reduce glass cracking. The tape was removed, and the electrodes were washed with water followed by sonicated in 0.2% Deconex 21 aqueous solution and acetone bath for 10 minutes each and dried at 400 °C for 15 minutes. For platinum electrodes: A thin layer of Pt-paste (Solaronix, Platisol T/SP) was slot printed with a punched Scotch tape piece on the conductive side. The electrodes were then heated at 450 °C for 10 minutes. A circular black mask (active area 0.15 cm^2) punched from black tape was used in the subsequent photovoltaic studies.

Dye-Sensitized Solar Cell assembly: The photoanode and counter electrode were sealed with a 25 μm or 60 μm thick hot melt gasket (Surlyn, Solaronix, "Meltonix 1170-25") by heating the system at 130 °C under a pressure of 0.2 psi for 1 minute with a sealing machine (Dyenamo, product DN-HM01). The electrolyte was added through the pre-drilled holes in the counter electrodes with the rubber sealing tip from a Solaronix "Vac'n'Fill Syringe" until the electrolyte began to emerge from the second counter electrode hole. The holes were sealed with a Surlyn sheet and a thin glass cover by heating at 130 °C under pressure (0.1 psi) for 25 seconds. Finally, soldered contacts were added with a MBR Ultrasonic soldering machine (model USS-9210) with

solder alloy (Cerasolzer wire diameter 1.6 mm, item # CS186-150). A circular black mask (active area 0.15 cm^2) punched from black tape was used in the subsequent photovoltaic studies.

In summary, TiO_2 electrodes are comprised of a 10 μm (**AP25**) and 15 μm (**AP25/D35**) film active layer of 20 nm TiO_2 nanoparticles with a 5 μm film scattering layer of >100 nm TiO_2 nanoparticles on top. The electrolyte is: 1.0 M DMII (1,3-dimethylimidazolium iodide), 0.5 M TBP (4-*tert*-butylpyridine), 0.03 M I_2, 0.1 M GuNCS (guanidinium thiocyanide) and LiI (lithium iodide) at 1.0 M or 0.7 M concentrations in acetonitrile:valeronitrile (85:15,v/v) solvent. TiO_2 electrodes were dipped in the dye solution for 20 hours.

5.3. Preparation of Cytop Solution and Deposition by Spin Coating

Cytop (CTL-809) was dissolved in 18 wt% concentration by dissolving it in CT-Sol.180 on hot plate which was set at 110 °C. The mixture was stirred for 5 minutes at 110 °C. After this the prepared mixture was spin coated (Laurel Model WS-650MZ-23) on the FTO in a continuous two step coating process with 500 rpm for 10 seconds and 1000 rpm for 20 seconds. At the end the FTO substrates were cured at 200 °C for 1 hour under ambient conditions in a programmable furnace (Vulcan® 3-Series model 3-550).

5.4. Photoanode Surface Treatment

PFTS treatment: **D35** Sensitized TiO_2 films were submerged in a 0.1 M solution of 97% 1H,1H,2H,2H-perfluorooctyltrimethoxysilane (PFTS) in hexanes for 90 minutes at 30 °C. The electrodes were rinsed with hexanes and assembled as described above.

5.5. Photocurrent Transient or Current Dynamic Studies

Current dynamic studies were made at varying light intensities with the same current-voltage curve generating light source and source meter in combination with an electronically controlled shutter (UNIBLITZ model# VMM-D1, electronically controlled filter wheel (THORLABS FW102C),

and custom written LabView Software to simultaneously control all components. The 6-position filter wheel was loaded with neutral density filters from Thor Labs allowing 79%, 50%, 32%, 10%, and 1% intensities of light to pass.

5.6. Electron Lifetime by Small Modulation Photovoltage Transient (SMPVT) Measurements

Electron lifetime measurements also known as small modulation photovoltage transient measurements were carried out with Dyenamo toolbox (DN-AE01). In this experiment the intensity of the light source is controlled by a modulating voltage on top of a bias voltage (LED light intensity). The open circuit voltage response is measured multiple times and averaged. The rise and decay times are calculated with the aid of the Levenberg-Marquard curve fitting algorithm. The carrier or electron lifetime of the solar cell is obtained from the averaging of rise and decay times. To the base light intensity was added a small square wave modulation (<10% intensity). With repetition frequency of 2 Hz, modulation amplitude of 10 mV and 1000 samples/second with averages of 5 were employed. The option for light off after every measurement was selected and bias voltages were 2.8, 2.85, 2.9, 2.95 and 3 V respectively for the LED light. The direction of illumination was always from the TiO_2 side and the device was 5 cm far from the LED light source. Electrochemical Impedance Spectroscopy: Electrochemical impedance spectroscopy (EIS) was measured in the dark with a bias at open circuit voltages measured through *J-V* measurements. The spectra were scanned in a frequency range of 10^{-1}–10^{5} Hz at room temperature. The alternating current (AC) amplitude was set at 10 mV.

6. EIS and SMPVT Results Discussion

Electrochemical impedance spectroscopy (EIS) in the dark and electron lifetime measurements by small modulation photovoltage transient method (Figure S4) were performed to

further analyze the optimized devices.[6] In EIS Nyquist plot, the radius of large semicircle increases in size directly with increase in the recombination resistance at TiO_2 oxide/electrolyte interface, whereas the small semicircle points to the resistance at counter electrode.[7] EIS of devices in Table 2 (main text) for Nyquist plot (Figure S4, a) shows the radius of semicircles in the order of device photovoltage i.e. **AP25/D35≈AP25/D35 CYTOP>AP25**, pointing to higher recombination resistance of co-sensitized devices. Electron lifetime measurements under open circuit voltage (V_{oc}) conditions, further confirmed the higher electron lifetime in TiO_2 for **AP25/D35** devices (Figure S4, b).[8] Co-sensitization leading to superior surface blocking properties is produced by **D35** due to its three dimensional and bulky butoxyl substituents.[1b, 8, 9] For Bode plot the max of the low frequency peak shifted towards left (Figure S4, d) for co-sensitized devices in accordance with Nyquist plot findings. Charge extraction measurements (Q_{oc}) at V_{oc} showed minimal change for **AP25** vs. **AP25/D35** devices in terms of CB shift (Figure S4, d).

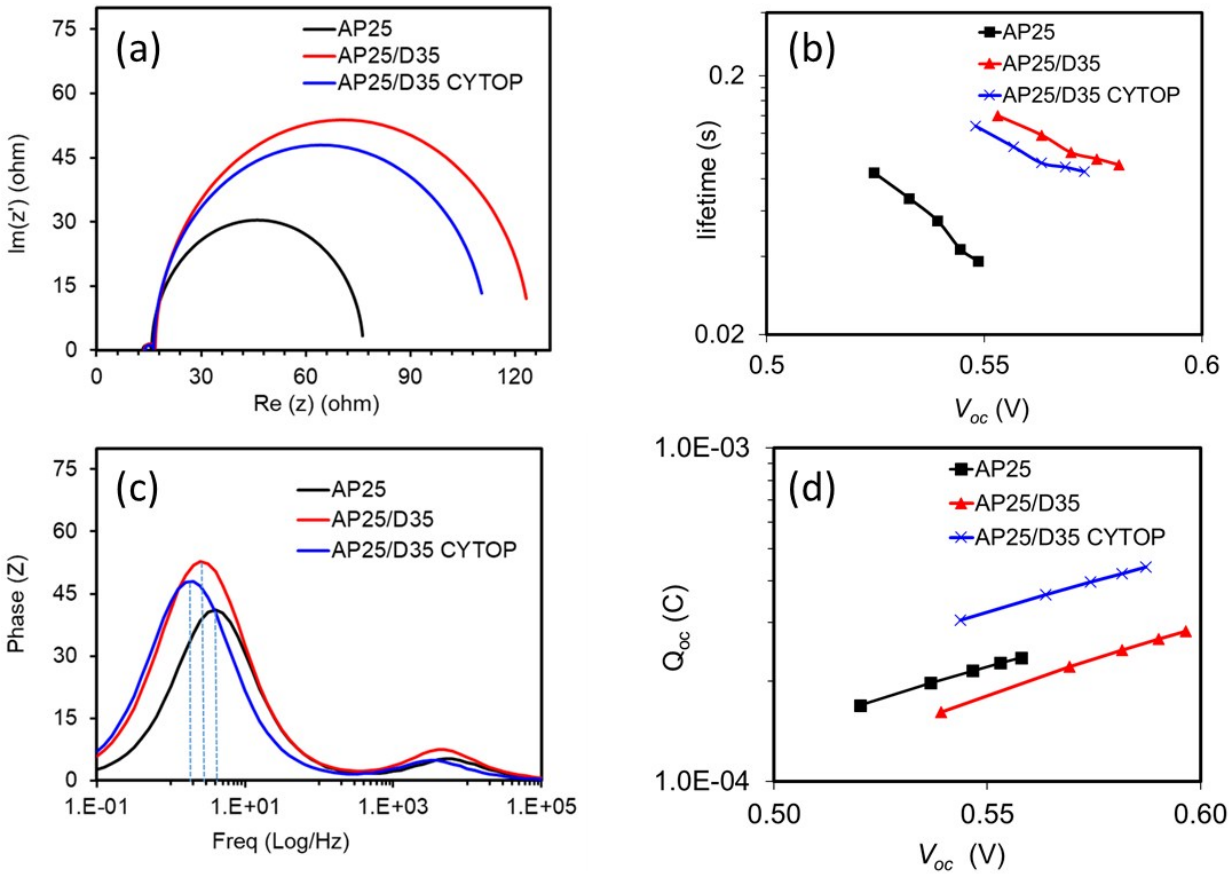

Figure S4. Comparison of best performing devices a) EIS Nyquist plot, b) photovoltage transient measurement for electron life c) EIS Bode plot, d) charge extraction measurements.

Device optimization strategies, such as chenodeoxycholic acid (CDCA) concentration optimizations led to an enhancement in the J_{sc} (19.9 vs. 17.3 mA/cm^2, max IPCE 75% vs. 65% at 580 nm, Fig. S5-S7) and V_{oc} (527 vs. 473 mV, Table S3) likely due to changing dye-dye surface interactions and slowing recombination losses.[8, 10] Focusing on **AP25** as a single dye in assembled DSCs, it was initially studied for dye solution and electrolyte additives such as chenodeoxycholic acid (CDCA) and 4-*tert*-butylpyridine (TBP).[8, 10] With only changing the chenodeoxycholic acid (CDCA) concentration (Figure S5, Table S3), **AP25** PCE was increased from 5.4% (no CDCA) to 6.8% PCE (40x CDCA, 26 % increase) accompanied by substantial increase in J_{sc} (19.9 vs. 17.3 mA/cm^2, max IPCE 75% vs. 65% at 580 nm, Figure S6-S7) and V_{oc} (527 vs. 473 mV, Table S3).

CDCA is a commonly employed adsorbent known to effect dye packing by occupying the space on TiO_2 between dye molecules, thus supporting efficient charge transport and recombination blocking at TiO_2 surface.[10-11] EIS confirmed the advantageous role of CDCA with increased recombination resistance and increased electron lifetime at 40x CDCA (Figure S8, Nyquist and Bode plots). Electron lifetime and Q_{oc} at V_{oc} conditions showed increased electron lifetime and marginal shift in conduction band with 40x CDCA present, respectively (Figure S9).

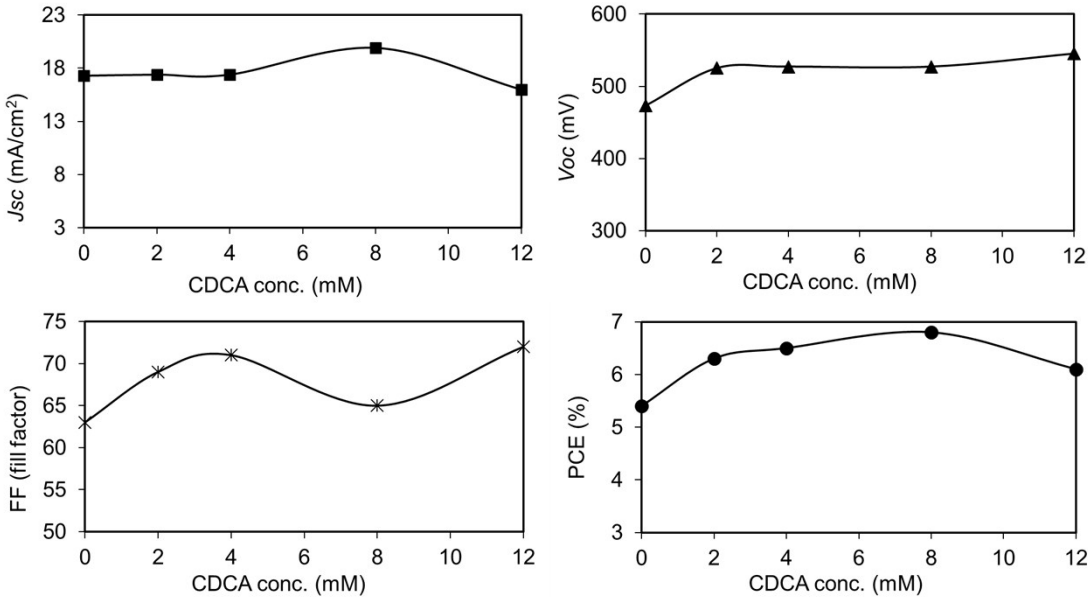

Figure S5. Effect of CDCA conc. on **AP25** devices with 0, 10, 20, 40, and 60 molar equivalents to the dye.

4-*tert*-butylpyridine (TBP) is a commonly employed basic electrolyte additive which is known to adsorb on TiO_2, increase V_{oc} and overall PCE (due to conduction band shift and increase in electron lifetime).[7] Contrary to this, LiI is known to lower the CB of TiO_2, with concomitant increase in electron injection and photocurrent response, particularly at longer wavelength.[12] At normal, 0.5 M concentration of TBP and 0.05 M Li^+ loading (LiI), **AP25** showed diminished J_{sc} (5.6 mA/cm^2) (Table S3, Figure S10). However, by increasing Li^+ loading in the electrolyte, IPCE

increased to 75% at 580 nm compared to only 25% (1 M LiI vs. 0.05 M LiI, Figure S12). Alternatively, the diminished photo response was recovered when TBP concentration was lowered to 0.1 M and Li^+ loading was kept at 0.05 M, pointing to known upward CB shift caused by TBP.[8] However at 0.1 M TBP concentration overall PCE was lower (5.4% vs. 6.8%) compared to when both higher TBP and Li^+ concentration was employed. Due to overall enhanced combined effect, **AP25** alone was further studied at 1 M LiI and 0.5 M TBP concentrations.

To circumvent the IPCE dip (400-550 nm) of **AP25** (Figure 2 (top), main text), co-sensitization with **D35** (complementary absorption compared to **AP25,** Figure S11 inset) was optimized through stepwise and cocktail staining methods (Table S4). Cocktail dye solution for **AP25:D35** (2:1) showed the overall best performance (7.3% vs. 7.2% PCE). To further fine tune the role of Li^+ doping **AP25/D35** sensitized devices were studied as function of LiI concentration (Table S5, Figure S12), TBP concentration was kept constant at 0.5 M. At 0.7 M LiI concentration, balanced J_{sc} and V_{oc} resulted in highest overall PCE of 7.8% compared to 6.3% (0.25 M LiI) and 7.3% (1.0 M LiI). Additionally, electron lifetime and charge extraction measurements (Figure S13) showed minimum to no favorable change in electron lifetime and conduction band shift for changing LiI concentration beyond 0.7 M. With optimized electrolyte at 0.7 M LiI and 0.5 M TBP, and cocktail solution for sensitization, TiO_2 active layer (20 nm particle size) film thickness was further studied to probe its effect on overall PCE.[13] **AP25/D35** devices were found to result in highest PCE at 15 μm active layer thickness (Table S6, 8.0 % PCE compared to 7.8% at 10 μm and 7.9% at 20 μm thickness), probably because of optimum dye loading.

To further elucidate the role of the individual **D35** and **AP25** dyes in the high performing co-sensitized devices and IPCE profile output, dye loading measurements (Fig. S15 and Table S8) were carried out. Though amount of **D35** was half that of **AP25** in the optimized concentrations

for dye dipping solutions (1:2) resulting in high photocurrent DSC devices, **D35** was estimated to be double the amount of **AP25** on the TiO_2 surface which is probably due to the relatively compact molecular size of **D35**. Additionally, preliminary photostability analysis (Fig. S16) of the **AP25**/**D35** device with a UV cutoff filter (>400 nm photons transmitted) shows a functional device for greater than 1000 hours with only a ~20% loss in PCE.

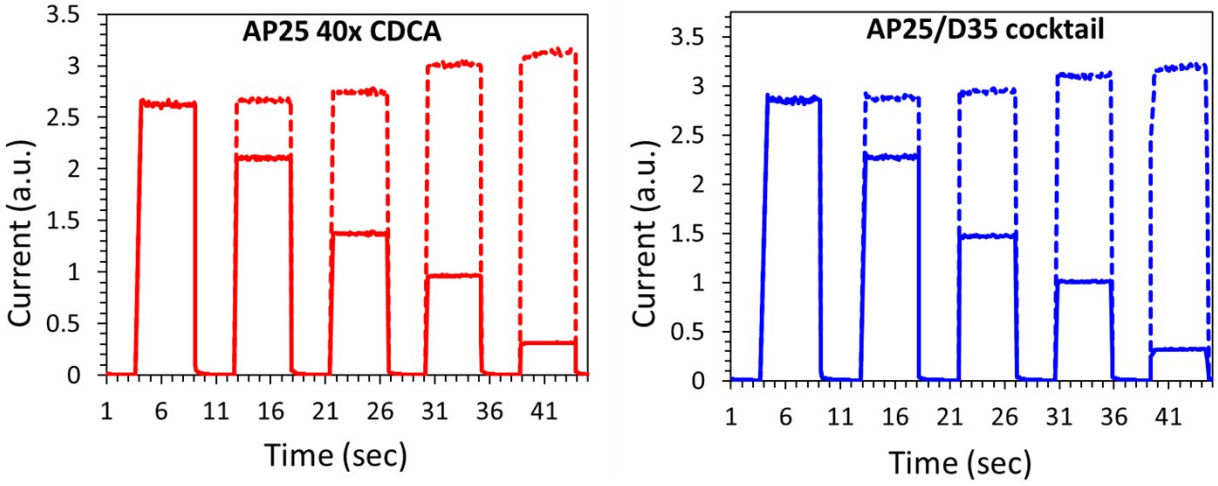

Figure S6. Comparison of current dynamics (CDs) behavior on TiO_2.

Table S3. Summary of DSC device performance parameters for **AP25** for CDCA and TBP study.[a]

Dye	LiI (M)	CDCA (mM)	TBP (M)	V_{oc} (mV)	J_{sc} (mA/cm^2)	J_{sc} (IPCE integrated)	FF (%)	PCE (%)
CDCA Study								
AP25	1.0	0 (0x)	0.5	473	17.3	16.0	63	5.4
	1.0	2.0 (10x)	0.5	525	17.4	16.1	69	6.3
	1.0	4.0 (20x)	0.5	527	17.4	15.9	71	6.5
	1.0	8.0 (40x)	0.5	527	19.9	18.3	65	6.8
	1.0	12.0 (60x)	0.5	545	16.0	14.7	72	6.1

TBP Study								
AP25	1.0	8.0 (40x)	0.5	527	19.9	18.3	65	6.8
	0.05	8.0 (40x)	0.5	506	5.6	4.9	68	1.9
	0.05	8.0 (40x)	0.1	461	19.1	17.9	63	5.4

[a]Device performances under AM 1.5G irradiation. TiO_2 electrodes are comprised of a 10 µm film active layer of 20 nm TiO_2 nanoparticles with a 5 µm film scattering layer of >100 nm TiO_2 nanoparticles on top. The electrolyte is: 1.0 M DMII (1,3-dimethylimidazolium iodide), 0.03 M I_2, 0.1 M GuNCS (guanidinium thiocyanide) in acetonitrile:valeronitrile (85:15,v/v) solvent (LiI and 4-*tert*-butylpyridine (TBP) concentration is as mentioned in the table). In the latter studies 40x CDCA was employed for **AP25** based devices and electrolyte with higher LiI loading (1.0 M except when mentioned) was termed as E2I.

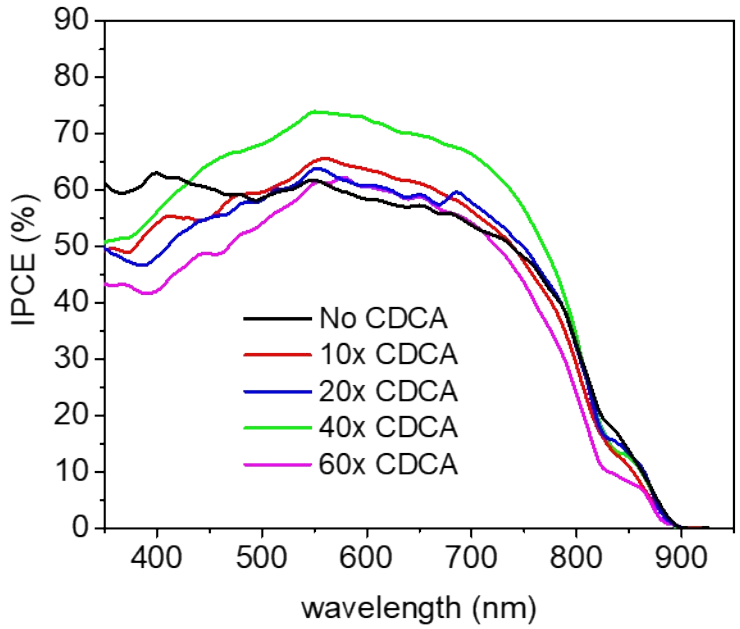

Figure S7. AP25 IPCE analysis as the function of CDCA concentration, 0, 10, 20, 40, and 60 molar equivalents to the dye.

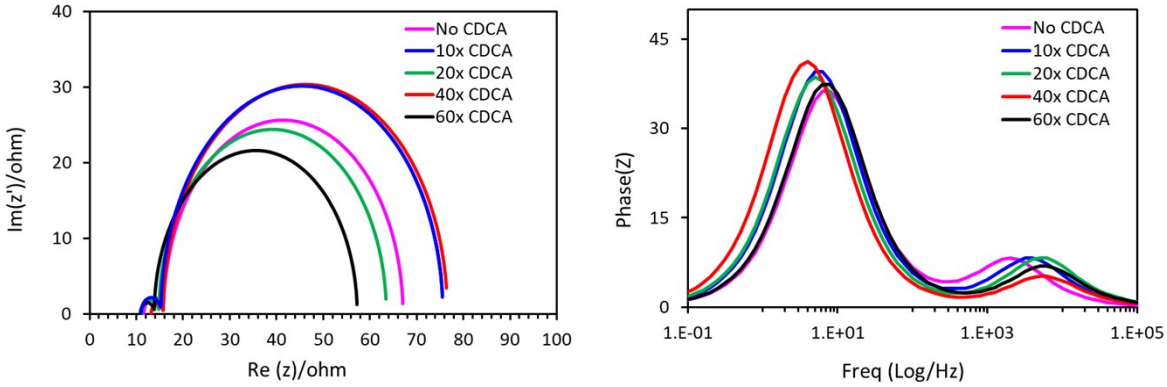

Figure S8. Effect of CDCA on EIS Nyquist (left) and Bode (right) plots of **AP25** based devices.

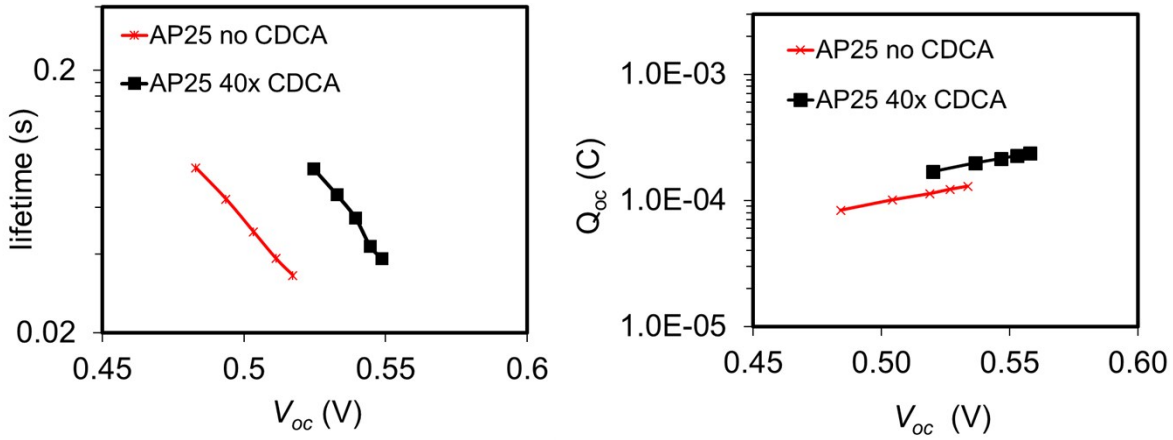

Figure S9. Effect of CDCA conc. on electron lifetime (left) and charge extraction (right) measurements of **AP25** devices.

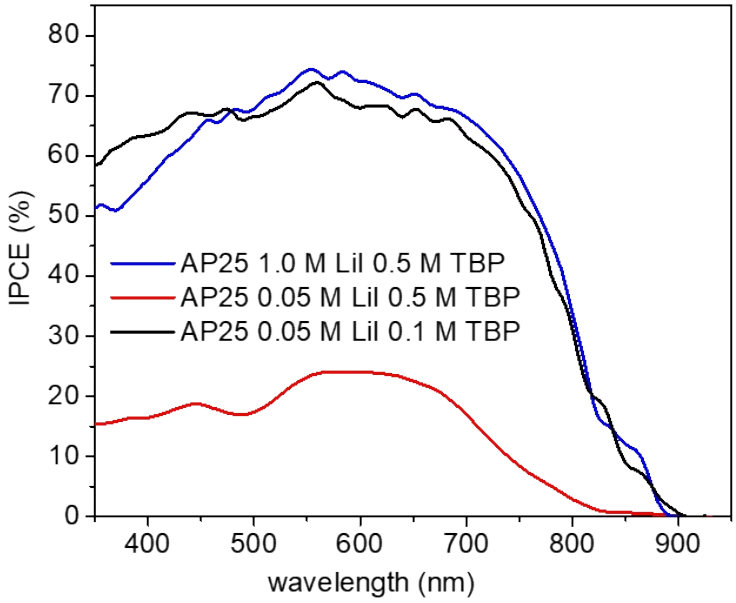

Figure S10. AP25 IPCE analysis as a function of TBP and LiI concentration.

Table S4. Summary of DSC performance parameters for **AP25/D35** co-sensitized devices.[a]

Dye	Dipping time (hourss)	V_{oc} (mV)	J_{sc} (mA/cm^2)	J_{sc} (IPCE integrated)	FF (%)	PCE (%)
D35	20	679	12.5	11.1	75	6.6
***Stepwise*[b]**						
AP25/D35	0.5	525	21.1	19.5	65	7.0
AP25/D35	1.5	571	18.7	17.5	70	7.2
***Cocktail*[c]**						
AP25/D35	20	565	21.4	20.8	62	7.3

[a]E2I as electrolyte was employed. [b]Before dipping into **D35** dye solution, electrodes were already stained with **AP25** (dipping of 20 hours). [c]Both **AP25** and **D35** (2:1) i.e. 0.2 mM **AP25** and 0.1 mM of **D35**, were dissolved together in ACN:ter. Butanol (1:1) with 9 mM of total CDCA. TiO_2 electrodes are comprised of a 10 µm film active layer of 20 nm TiO_2 nanoparticles with a 5 µm film scattering layer of >100 nm TiO_2 nanoparticles on top.

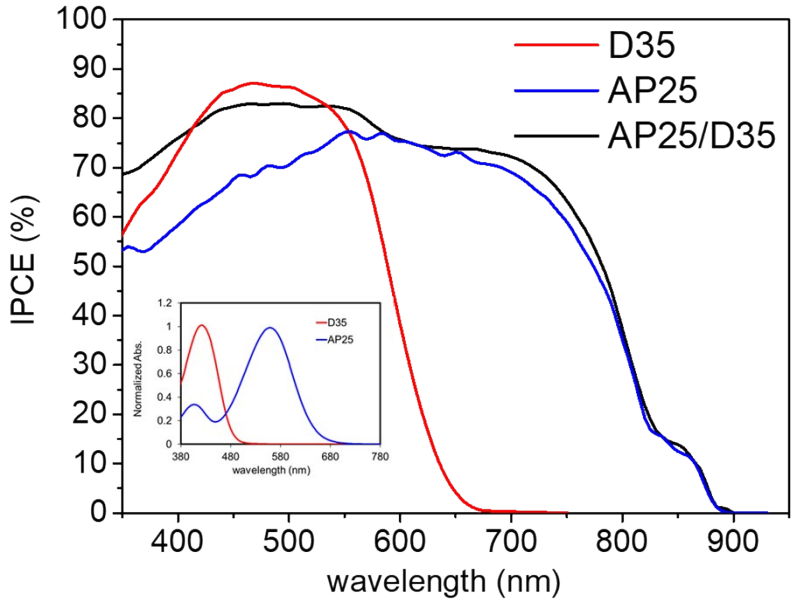

Figure S11. IPCE comparison of **D35**, **AP25** and **AP25/D35,** devices all at 1 M LiI concentration, inset solution absorption comparison of **D35** and **AP25**.

Table S5. Summary of DSC performance parameters for **AP25/D35** devices for LiI study.[a]

Dye	LiI (M)	V_{oc} (mV)	J_{sc} (mA/cm^2)	J_{sc} (IPCE integrated)	FF (%)	PCE (%)
AP25/D35	0.25	641	14.0	13.5	70	6.3
	0.5	646	16.1	15.5	72	7.4
	0.7	584	20.2	19.2	66	7.8
	1.0	565	21.4	20.8	62	7.3

[a] Cocktail solution of **AP25/D35** with 9 mM CDCA was employed. **AP25:D35** ratio of 2:1 was employed. TiO_2 electrodes are comprised of a 10 µm film active layer of 20 nm TiO_2 nanoparticles with a 5 µm film scattering layer of >100 nm TiO_2 nanoparticles on top.

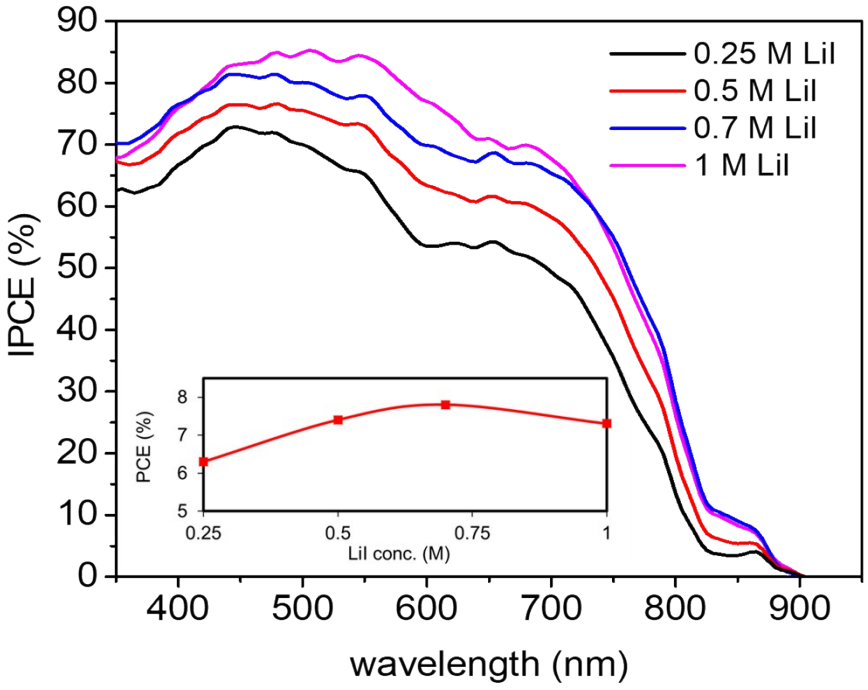

Figure S12. IPCE comparison of **AP25/D35** devices for LiI concentration study, inset shows the PCE of device as function of LiI conc.

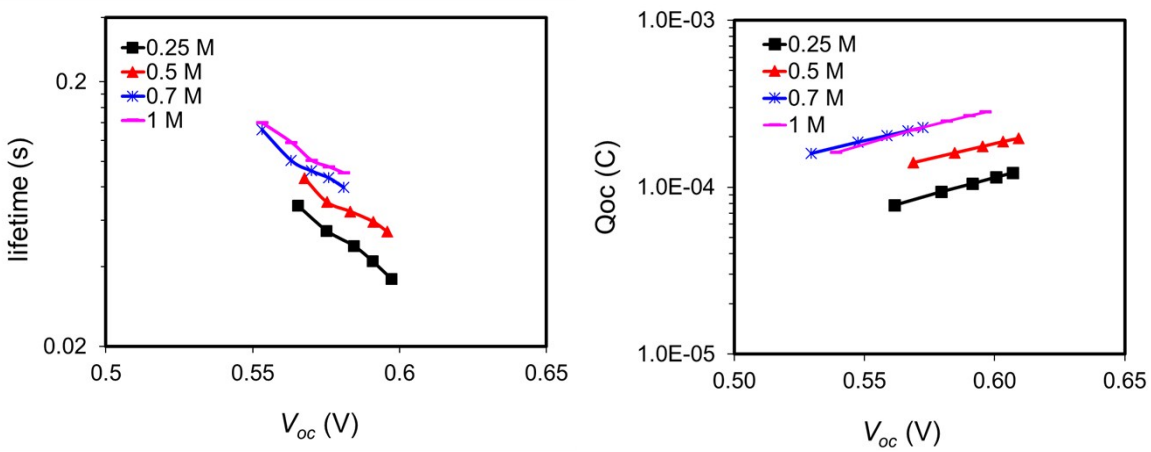

Figure S13. Effect of LiI conc. on electron lifetime (left) and charge extraction measurements of **AP25/D35** (right) co-sensitized devices.

Table S6. Summary of DSCs performance parameters for **AP25/D35** devices, TiO_2 thickness optimization and CYTOP effect.[a]

Dye	TiO_2 thickness (µm)	V_{oc} (mV)	J_{sc} (mA/cm^2)	FF (%)	PCE (%)
TiO_2 active layer thickness optimization					
AP25/D35	10	584	20.2	66	7.8
	15	564	21.4	67	8.0
	20	545	23.2	63	7.9
Effect of CYTOP (antireflection coating)					
AP25/D35 (device #1)	20	551	24.5	63	8.4
AP25/D35 (device #2)	20	578	24.0	62	8.5
AP25/D35 (device #3)	20	565	22.8	63	8.0
AP25/D35 (Avg.)	20	570±11	23.7±0.7	63±0.5	8.3±0.2

[a]All the devices have a 5 µm scattering layer with >100 nm TiO_2 nanoparticles. The **AP25/D35** iodine electrolyte was employed: 1.0 M DMII (1,3- dimethylimidazolium iodide), 0.7 M LiI, 30 mM I_2, 0.5 M TBP, 0.1 M GNCS (guanadinium thiocyanate) in acetonitrile and valeronitrile (v/v, 85/15).

7. Device comparison with N719 and Black Dye

Table S7. Summary of DSCs device data for **AP25/D35** with **Black Dye** and **N719**.

Entry	Dye	Type	J_{sc} (mA/cm^2)	J_{sc} (IPCE integrated)	V_{oc} (mV)	FF (%)	PCE (%)	IPCE at 500 nm (%)
Delcamp lab @ University of Mississippi								
1	**AP25/D35***	Organic	24.5	23.4	551	63	8.4	86
2	**Black Dye***	Precious metal Ru (II)	20.8	20.1	638	72	9.7	75
3	**N719***	Precious metal Ru (II)	17.4	16	712	74	9.6	80
Few examples of high J_{sc} (>20 mA/cm^2) sensitizers for DSCs from literature[14]								
4	**Dye 2**	Precious metal Os (II)	23.7	---	0.32	36	2.7	75
5	**HD-1-mono**	Precious metal Os (II)	21.4	---	0.55	60	7.06	82
6	**DX1**	Precious metal Ru (II)	26.8	---	0.53	54	7.7	86
7	**DX3**	Precious metal Ru (II)	30.3	---	0.56	60	10.2	88
8	**TF-52**	Precious metal Os (II)	23.3	---	0.60	63	8.85	76
9	**LG5**	Zn porphyrin	21.0	---	0.68	71	10.2	85
10	**ZL003**	Organic	20.7	---	0.956	69	13.6	90

*TiO_2 thickness (active + scatter layer) was 15+5 µm, 30+5 µm and 20+5 µm. Active layer of all the electrodes were prepared by Dyesol-18NRT paste. Entry 1 and 2, applied CYTOP coating. . The electrolyte for **AP25**/**D35** is: 1.0 M DMII (1,3-dimethylimidazolium iodide), 0.03 M I_2, 0.1 M GuNCS (guanidinium thiocyanide), 0.7 M LiI, 0.5 M TBP in acetonitrile:valeronitrile (85:15,v/v) solvent. The electrolyte for Black Dye is: 1.0 M DMII (1,3-dimethylimidazolium iodide), 0.03 M I_2, 0.1 M GuNCS (guanidinium thiocyanide), 0.1 M LiI, 0.3 M TBP in acetonitrile:valeronitrile (85:15,v/v) solvent. The electrolyte for **N719** is: 1.0 M DMII (1,3-dimethylimidazolium iodide), 0.03 M I_2, 0.1 M GuNCS (guanidinium thiocyanide), 0.05 M LiI,

0.5 M TBP in acetonitrile:valeronitrile (85:15,v/v) solvent. Ru stand for ruthenium and Os stands for osmium.

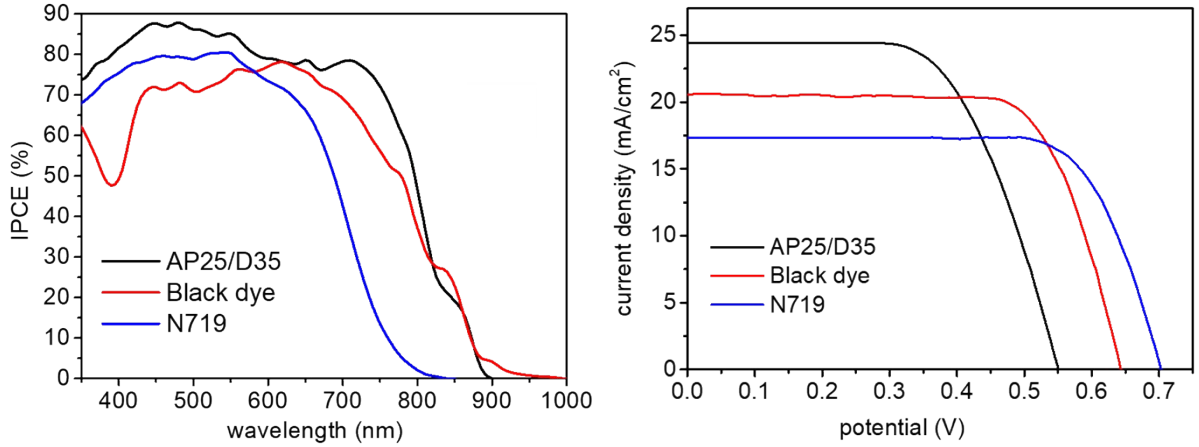

Figure S14. IPCE (left) and *J-V* (right) comparison of **AP25/D35** with **Black dye** and **N719**.

8. Dye Loading Measurements

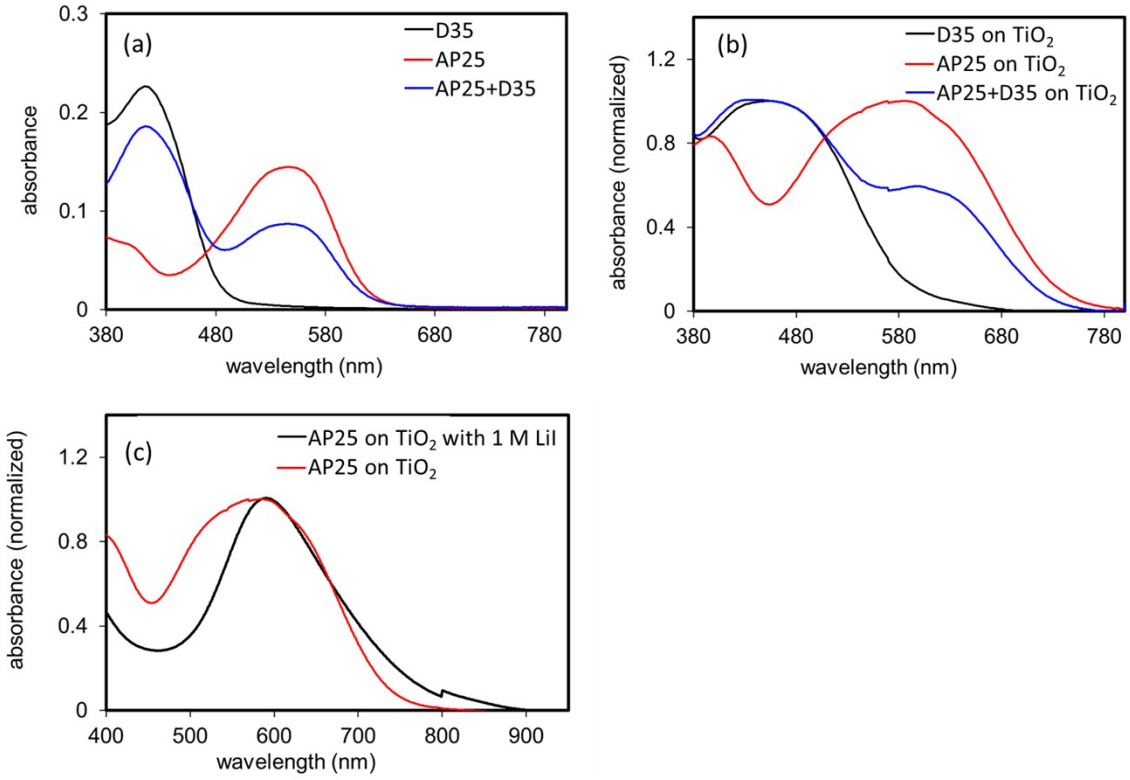

Figure S15. UV-Vis absorption of desorbed dye solutions (a) and stained TiO_2 electrodes (b), TiO_2 film photoabsroption comparison with and without electrolyte additive LiI (c). The desorption solvent is 0.01 M tetrabutylammonium hydroxide (TBAOH) in DMF from 2.5 µm films of TiO_2, which were stained exactly as described for the DSC devices prepared in this manuscript.

Table S8. Dye loading density studies as determined through desorption from photoanodes with 0.01 M TBAOH in DMF.

Dye	*Loading Density (mol/cm²)*
From single dye TiO_2	
D35	8.69×10^{-6}
AP25	4.60×10^{-6}
Y123[a]	1.14×10^{-5}
MK2	1.77×10^{-5}
B11[b]	8.16×10^{-6}
From Co-sensitized (AP25/D35) TiO_2	
D35	5.96×10^{-6}
AP25	2.78×10^{-6}

[a]dye dipping solution for **Y123** 0.3 mM in MeCN:ter. butanol (1:1) with 50x CDCA. [b]dye dipping solution for **B11** was MeCN:tert-butanol:DMSO (1:1:1) with 10x CDCA .

9. Photostability Data

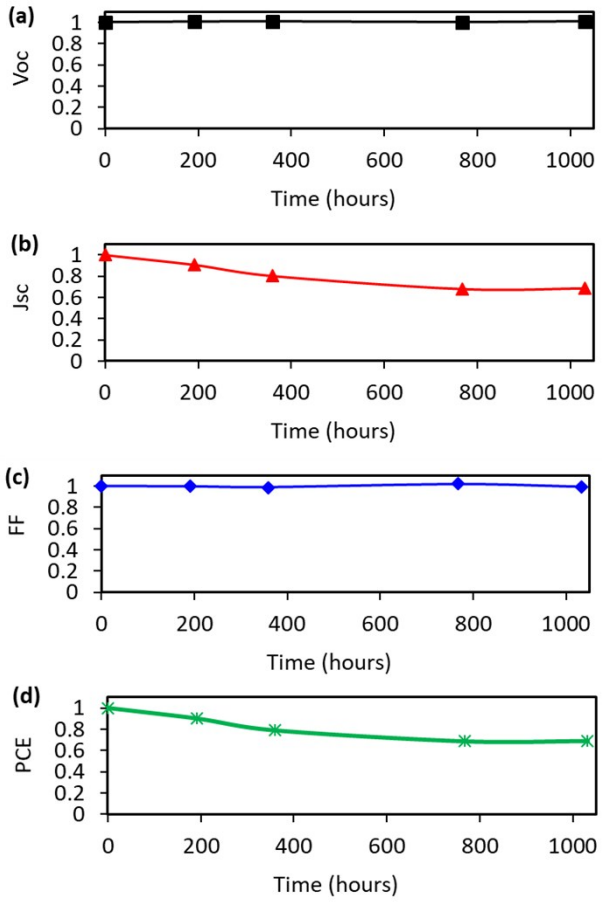

Figure S16. DSC device stability studies with **AP25/D35** during 1000 hours of continuous illumination with initial parameter values normalized to 1. Note: A 400 nm adhesive UV filter film from Solaronix was used in front of the devices.

9. Illustrative figure for AP25 application in SSM-DSCs

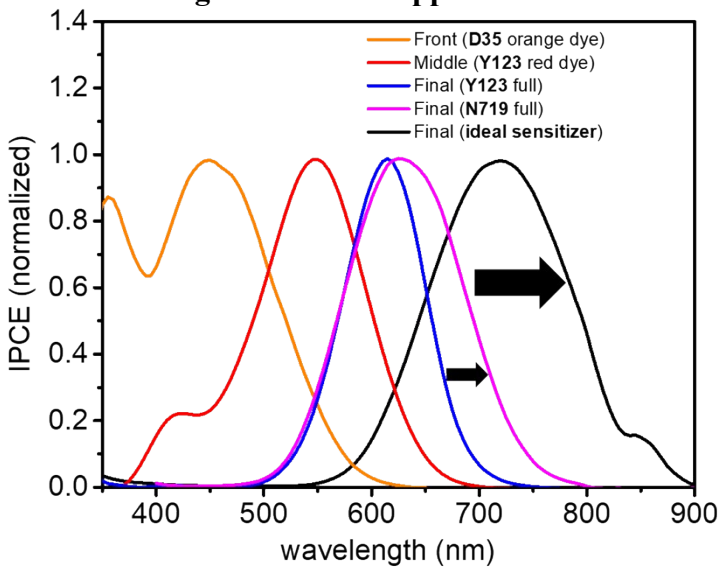

Figure S17. IPCE graphs of individual devices in the stack of 3-subcell SSM-DSCs, comparison for the role of back cell in harvesting NIR photons. [15] "full" refers to the device with the scattering layer.

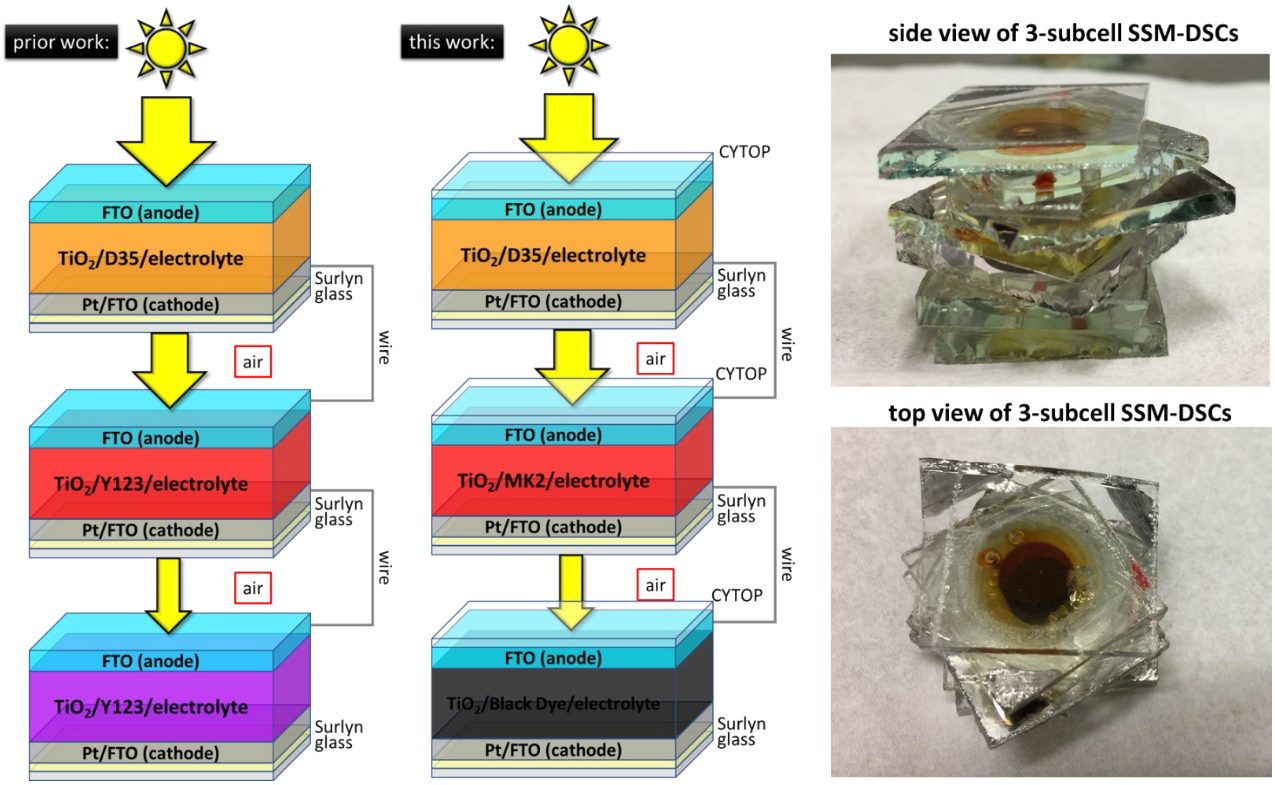

Figure S18. Illustrative figures summarizing the interfaces in 3-subcell SSM-DSC (left and middle), real image of mechanically stacked 3-subcell SSM-DSCs (right).

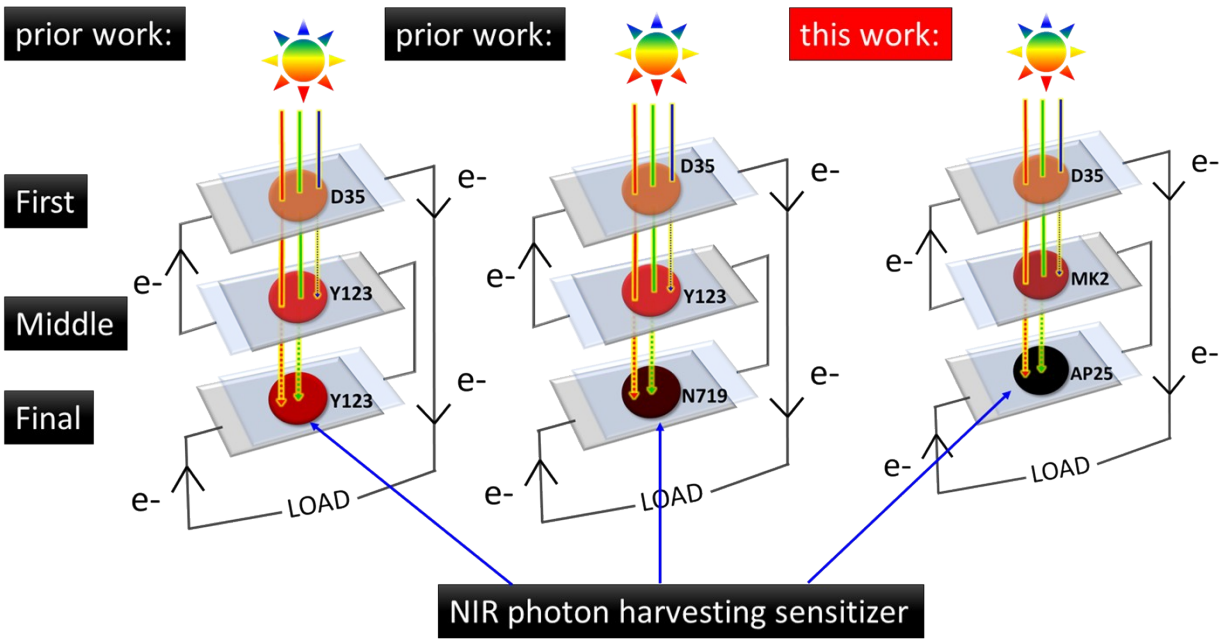

Figure S19. Illustration depicting the introduction of **AP25** as an efficient NIR organic sensitizer for 3-subscell SSM-DSCs.

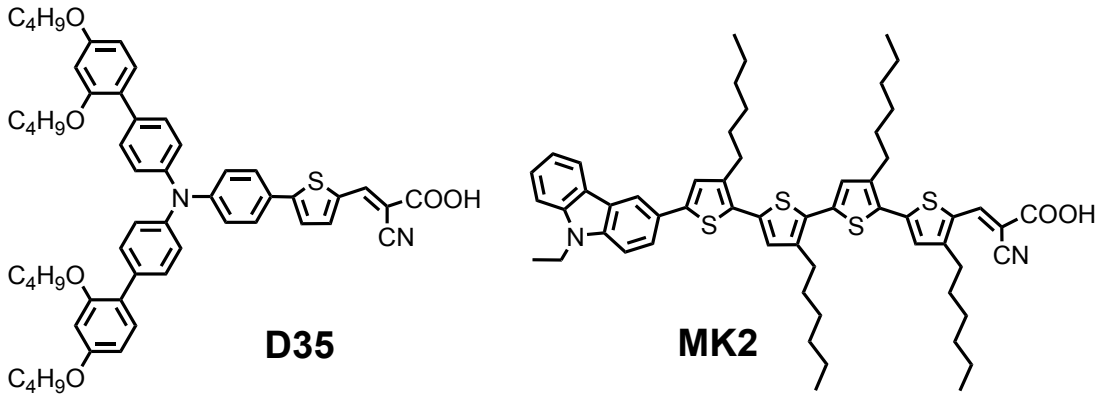

Figure S20. Chemical structures of **D35** and **MK2**.[16]

Table S9. Individual DSC performance parameters for various dyes and varying film thicknesses.[a]

Dye	TiO_2 thickness (µm)	V_{oc} (mV)	J_{sc} (mA/cm^2)	FF (%)	PCE (%)
D35	1.8	835±2	7.0±0.1	71±1	4.1±0.1
	5	899±38	9.6±0.3	71±2	6.1±0.3
MK2	3.5	776±8	13.8±0.3	71±1	7.5±0.2
Full	20	570±11	23.7±0.7	63±1	8.3±0.2

[a] **D35** and **MK2** DSCs were made from terpinol diluted P30 (particle size: 30 nm, Dyenamo, DN-GPS-30TS) paste. For **D35** and **MK2,** a cobalt based electrolyte was used:0.25 M $Co(bpy)_3(PF_6)_2$, 0.05 M $Co(bpy)_3(PF_6)_3$, 0.1 M LiTFSI, and 0.5 M 4-*tert*-butylpyridine (TBP), in acetonitrile. For **AP25/D35** iodine electrolyte was employed: 1.0 M DMII (1,3-dimethylimidazolium iodide), 0.7 M LiI, 30 mM I_2, 0.5 M TBP, 0.1 M GNCS (guanadinium thiocyanate) in acetonitrile and valeronitrile (v/v, 85/15). All cells had CYTOP coatings. **D35** devices additionally had F-SAM treatment. **MK2** dye solution (0.3 Mm) was prepared in toluene and electrodes were dipped for 6 hours. "Full" indicates **AP25/D35** co-sensitized subcell with 15 µm TiO_2 active layer and a 5 µm TiO_2 scattering layer.

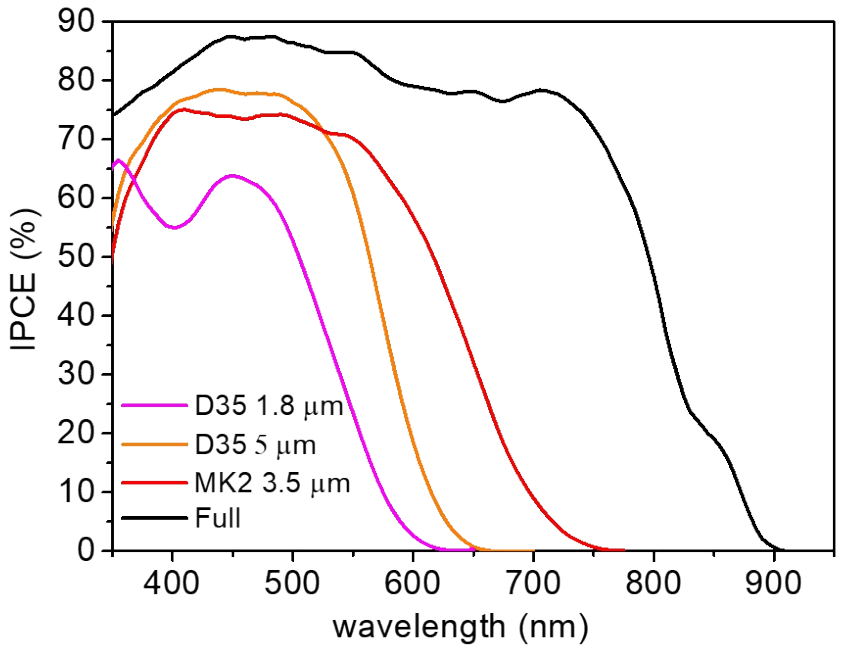

Figure S21. IPCE spectrum of individual devices employed in **SSM-DSCs**.

Table S10. SSM-DSC performance parameters with CYTOP for varying dyes and varying film thicknesses.[a]

device	Thickness (µm)	V_{oc} (mV)	J_{sc} (mA/cm^2)	FF (%)	PCE (%)
2 subcell SSM-DSC devices					
D35/Full	5/10	1467±35	9.9±0.24	69±1	10.1±0.2
3 subcell SSM-DSC devices					
D35/MK2/Full	1.8/3.5/full	2132±21	6.4±0.4	71±2	9.5±0.5

[a]For **D35** and **MK2** a cobalt based electrolyte was used:0.25 M $Co(bpy)_3(PF_6)_2$, 0.05 M $Co(bpy)_3(PF_6)_3$, 0.1 M LiTFSI, and 0.5 M 4-*tert*-butylpyridine (TBP), in acetonitrile. For "**Full**" iodine electrolyte was employed: 1.0 M DMII (1,3- dimethylimidazolium iodide), 0.7 M LiI, 30 mM I_2, 0.5 M TBP, 0.1 M GNCS (guanadinium thiocyanate) in acetonitrile and valeronitrile (v/v, 85/15). "Full" indicates **AP25/D35** co-sensitized subcell with 15 µm TiO_2 active layer and a 5 µm TiO_2 scattering layer.

Table S11. SSM-DSC performance parameter details for individual and in stack devices.

dye and TiO_2 thickness (µm)	**Position**	**V_{oc} (mV)**	**J_{sc} (mA/cm^2)**	**FF (%)**	**PCE (%)**
D35/Full					
D35 5 µm	front	899±38	9.6±0.3	71±2	6.1±0.3
AP25/D35 full	itself	569.5±11	23.7±0.7	63±1	8.3±0.2
	2nd	578±2	9.9±0.4	74±1	4.1±0.2
D35/Full (5/full)	**Tandem**	**1467±35**	**9.9±0.2**	**69±1**	**10.1±0.2**
D35/MK2/Full					
D35 1.8 µm	front	835±2	7.0±0.1	71±1	4.1±0.1
MK2 3.5 µm	itself	776±8	13.8±0.3	71±1	7.5±0.2
	2nd	756±1	6.9±0.4	77±1	3.8±0.4
Full	itself	570±11	23.7±0.7	63±1	8.3±0.2
	3rd	567±11	6.2±0	77±1	2.7±0.1
D35/MK2/Full (1.8/3.5/full)	**Tandem**	**2132±21**	**6.3±0.4**	**71±2**	**9.5±0.5**

"Full" indicates **AP25/D35** co-sensitized subcell with 15 µm TiO_2 active layer and a 5 µm TiO_2 scattering layer. "itself" is the device when measured out of the **SSM-DSCs** configuration. 2nd and 3rd refers to measurement in the **SSM-DSC** configuration.

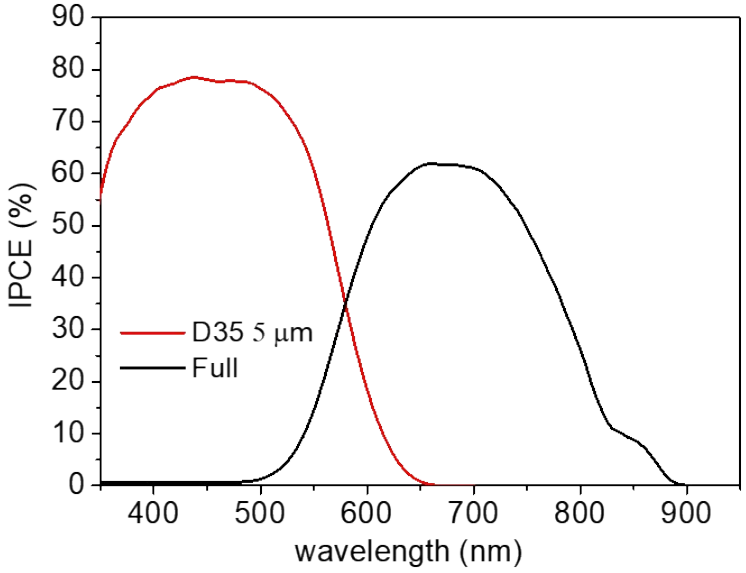

Figure S22. IPCE spectrum of individual devices measured while in a 2 device **SSM-DSCs** configuration.

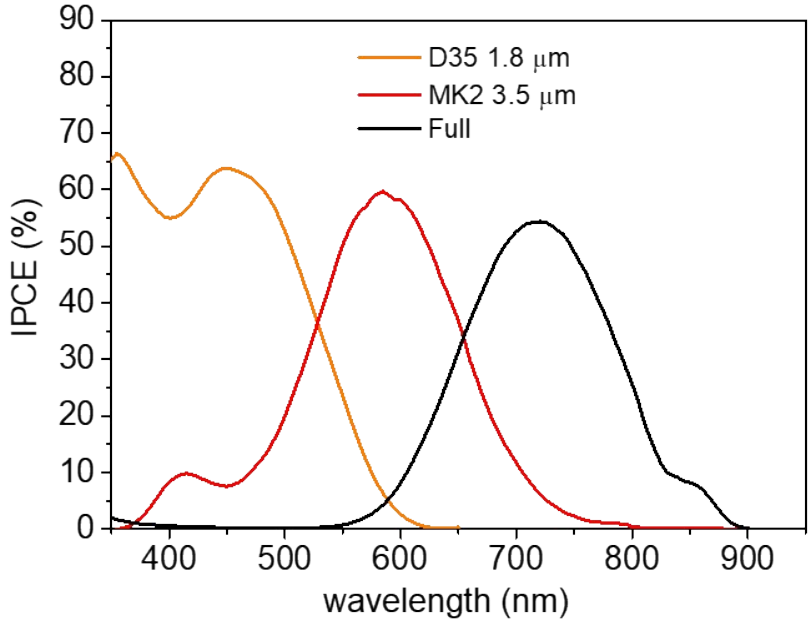

Figure S23. IPCE spectrum of individual devices when measured while in 3 device **SSM-DSCs** configuration.

11. NMR Spectrums

Figure

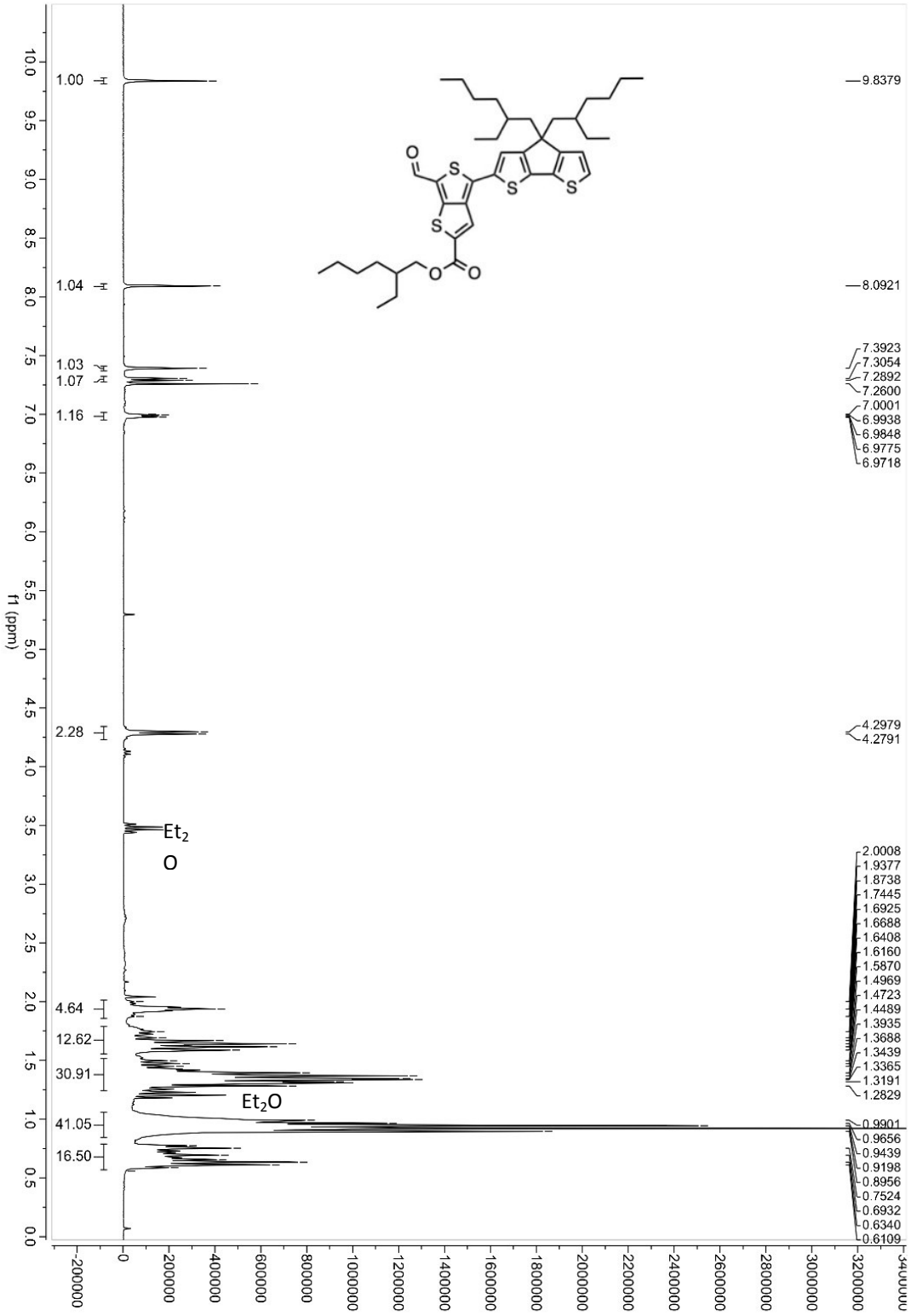

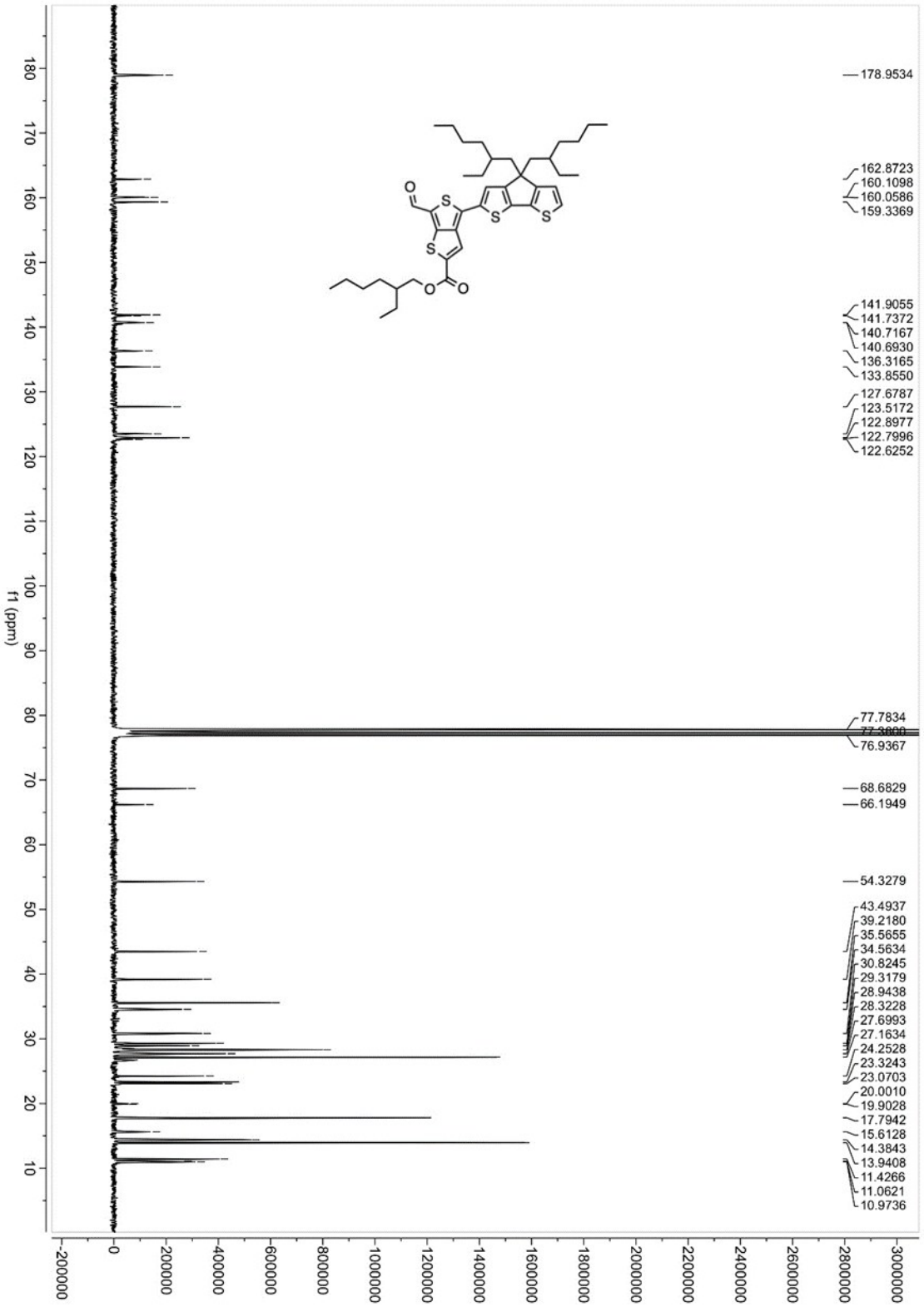

Figure S25. Compound **3**: ^{13}C NMR ($CDCl_3$), 75 MHz

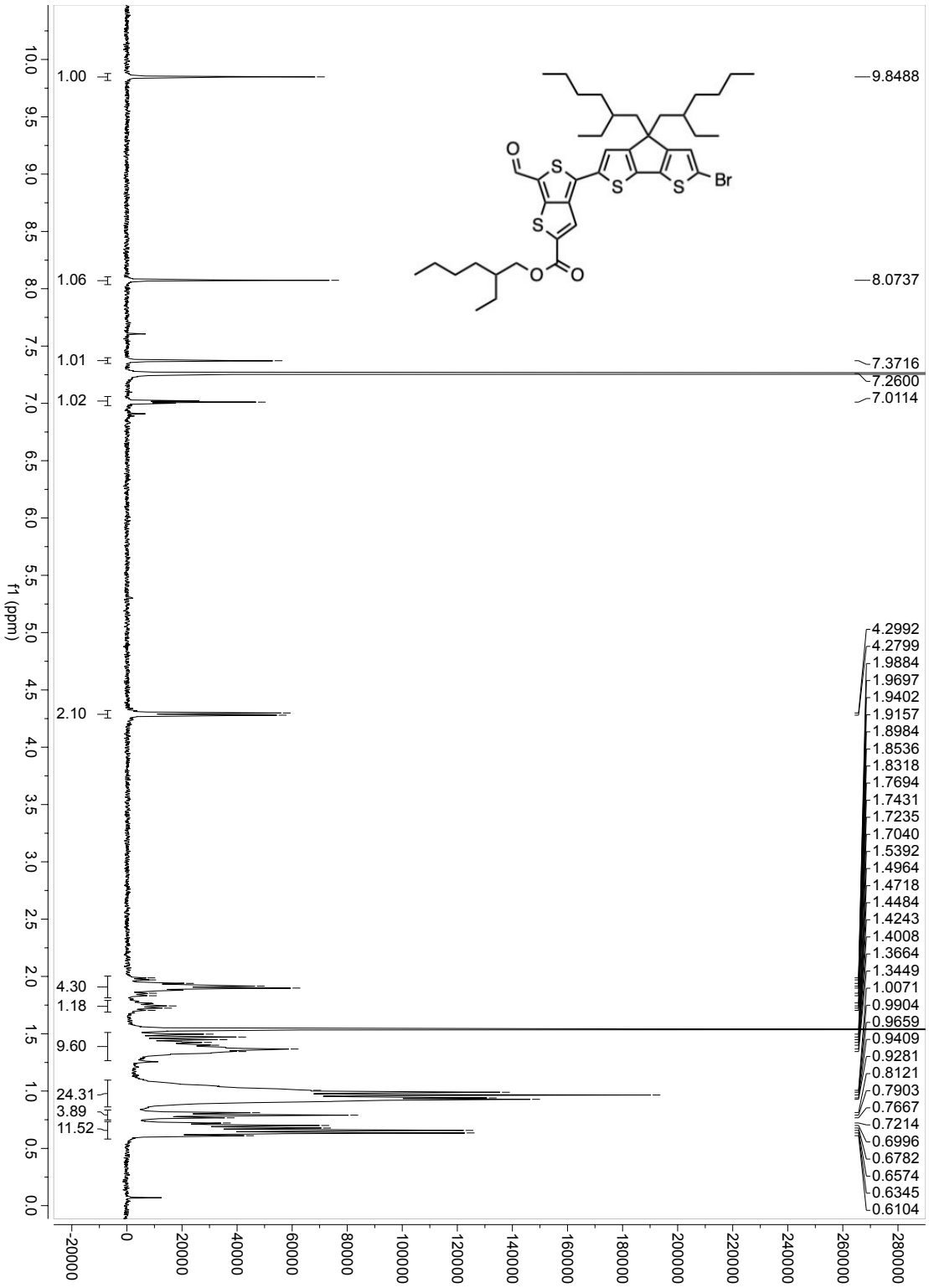

Figure S26. Compound **4**: ^{1}H NMR ($CDCl_3$), 300 MHz

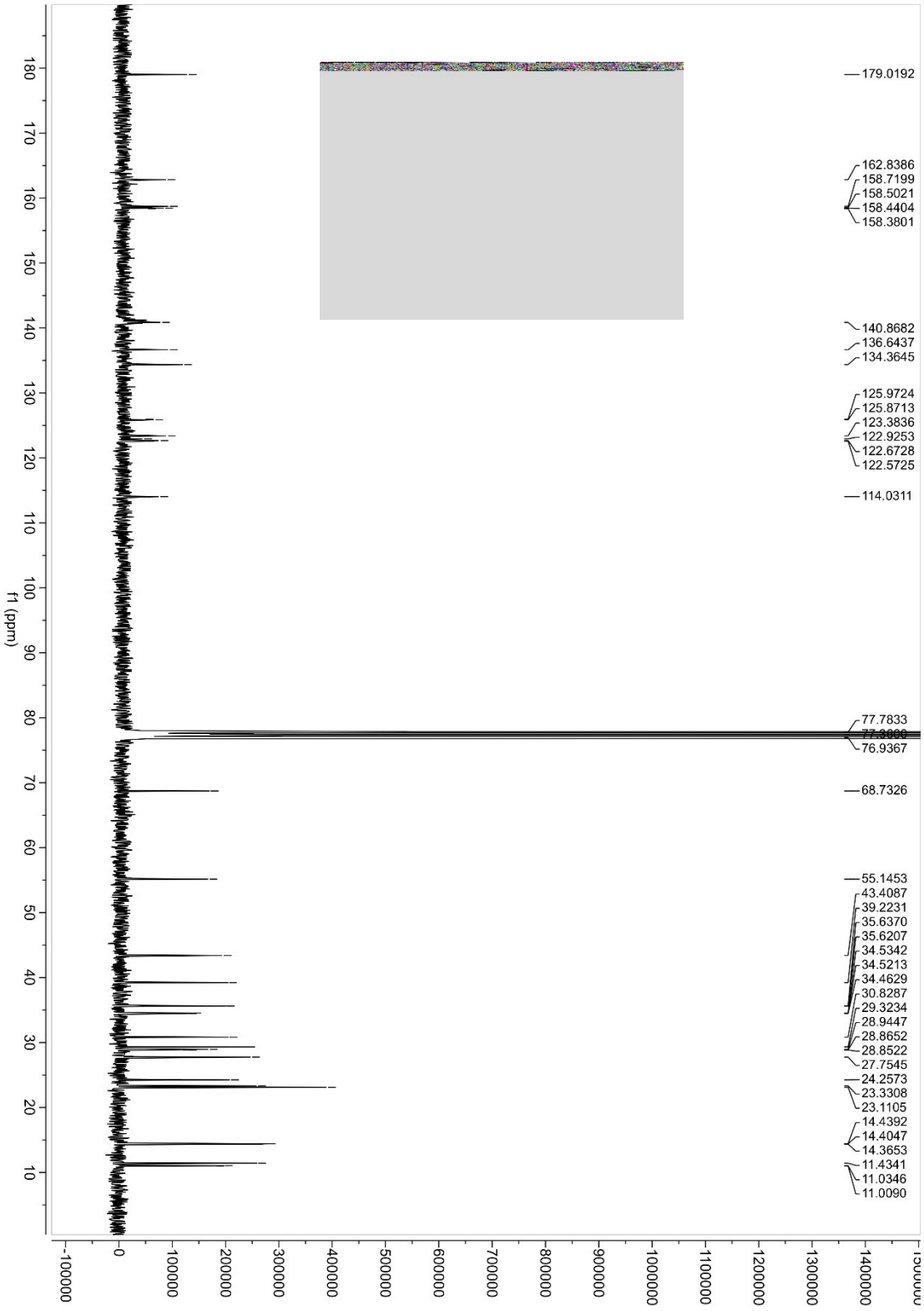

Figure S27. Compound **4**: ^{13}C NMR ($CDCl_3$), 75 MHz

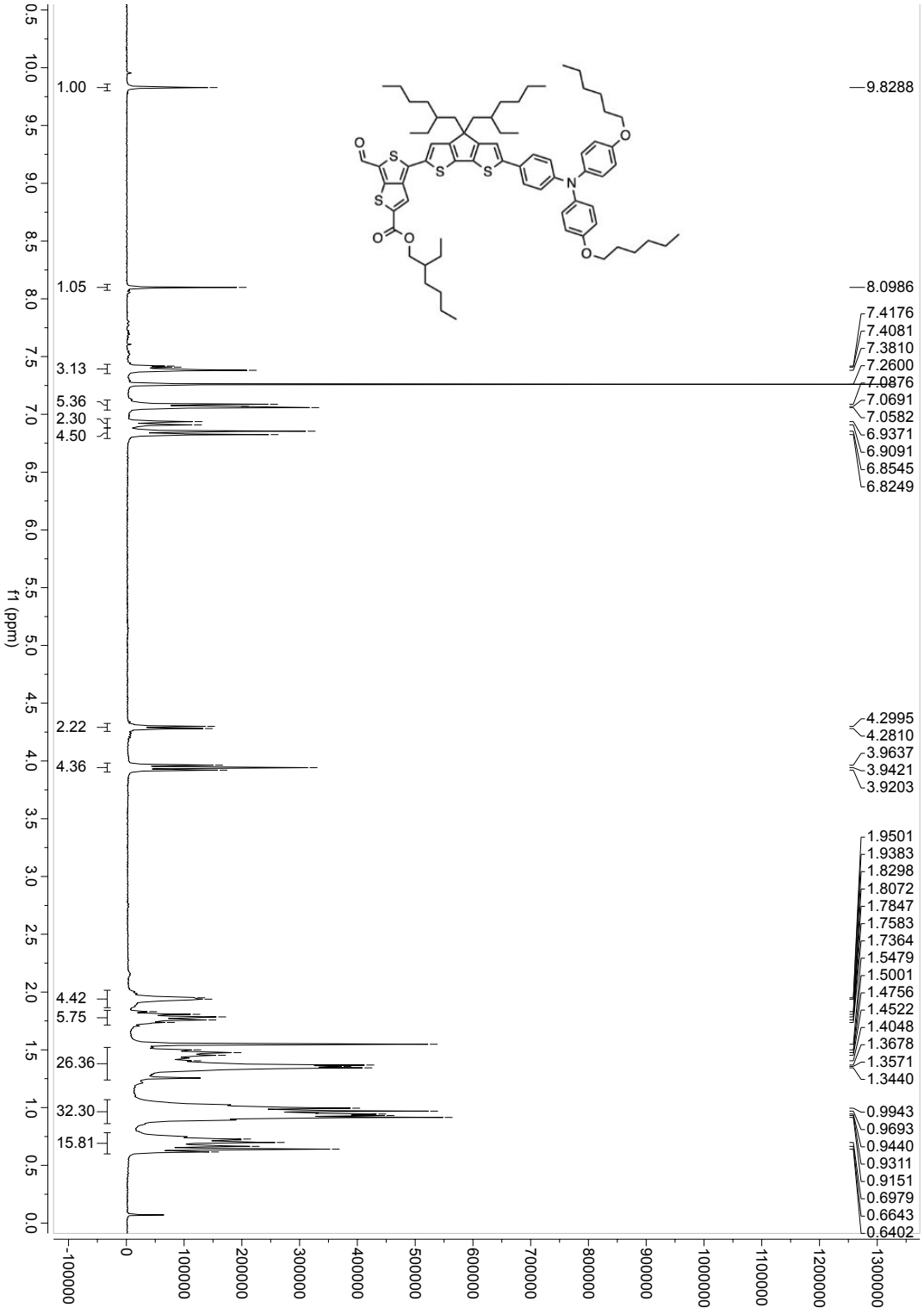

Figure S28. Compound **5**: ^{1}H NMR ($CDCl_3$), 300 MHz

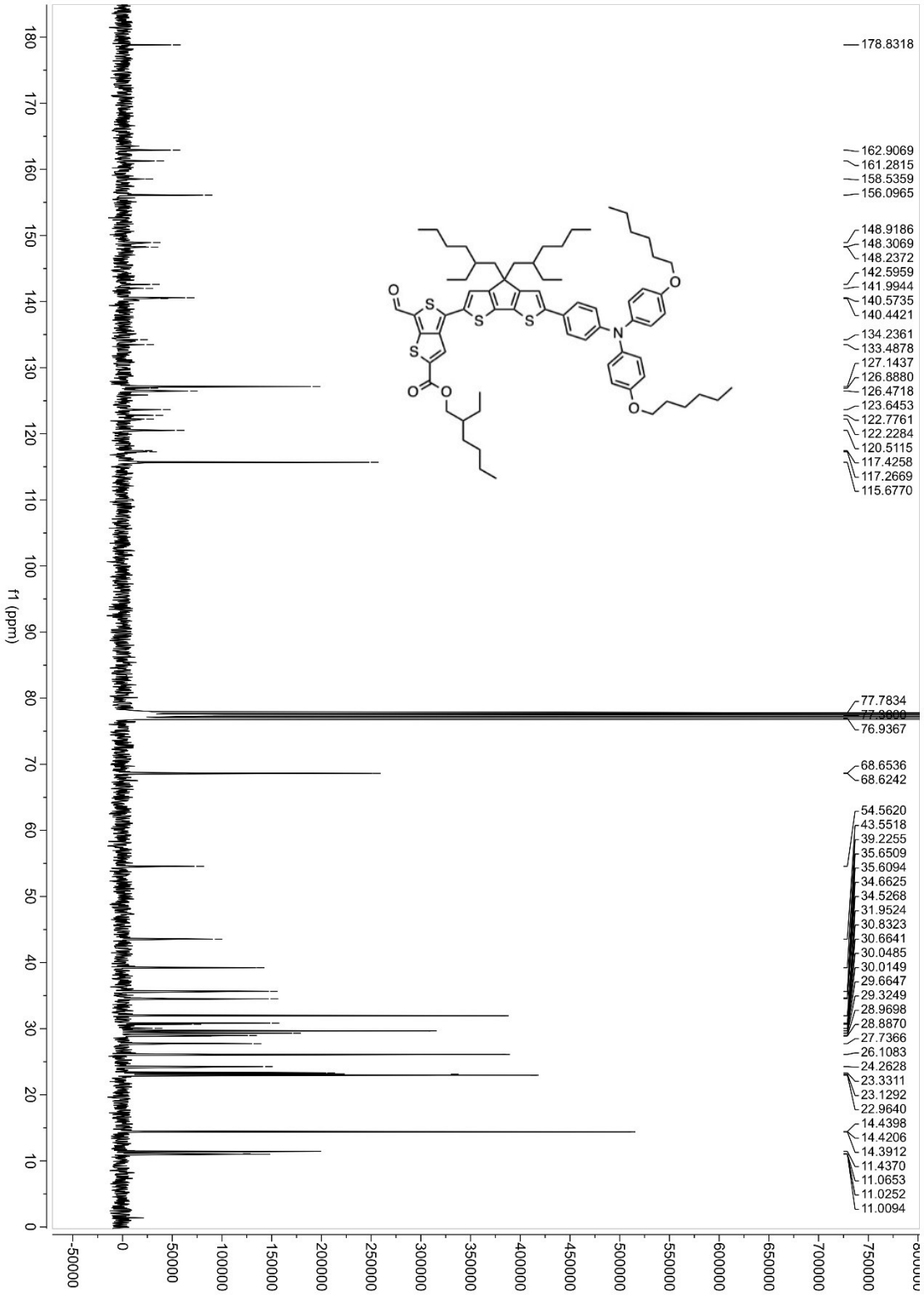

Figure S29. Compound **5**: ^{13}C NMR ($CDCl_3$), 75 MHz

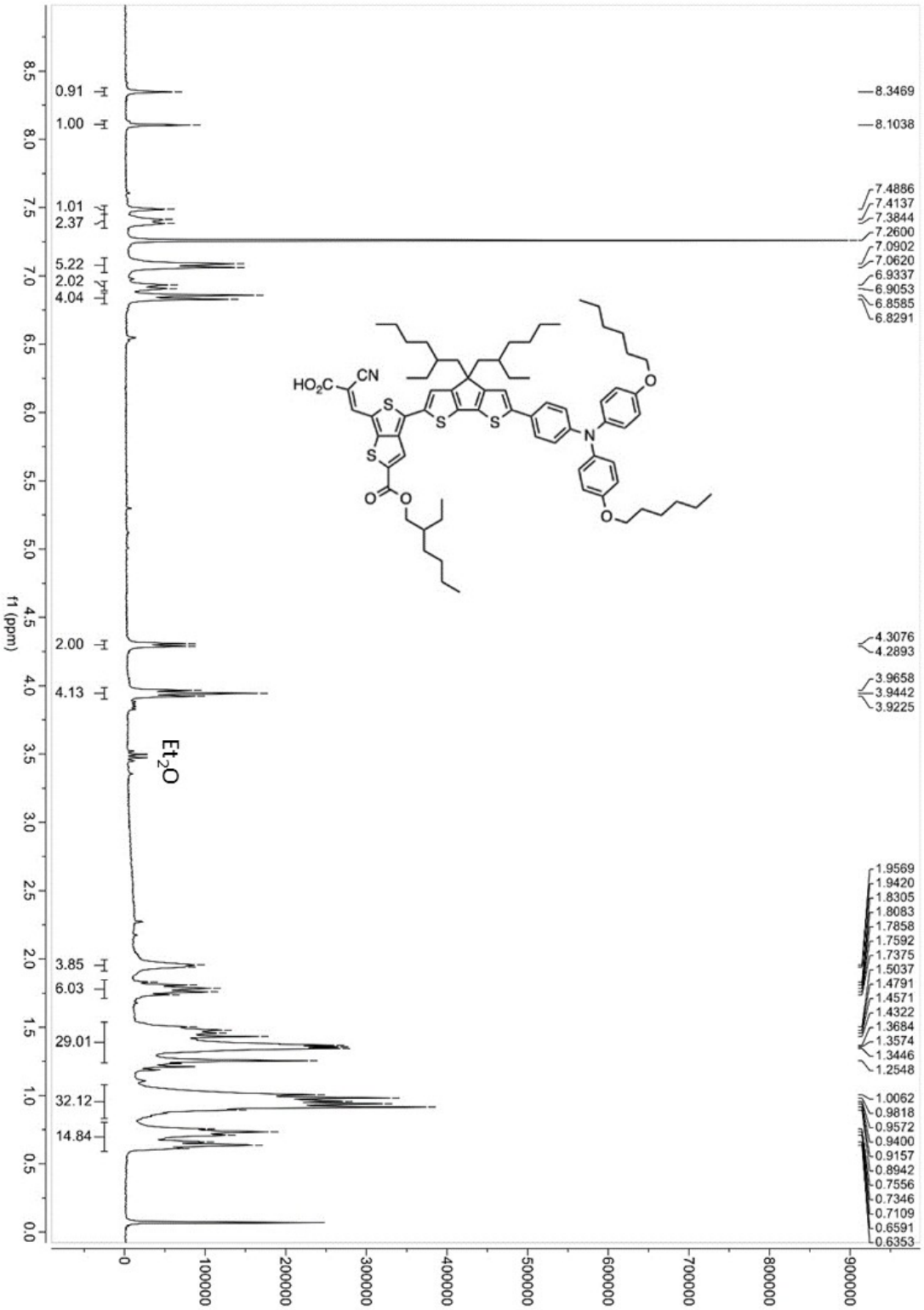

Figure S30. Compound **6** (a): ^{1}H NMR ($CDCl_3$), 300 MHz

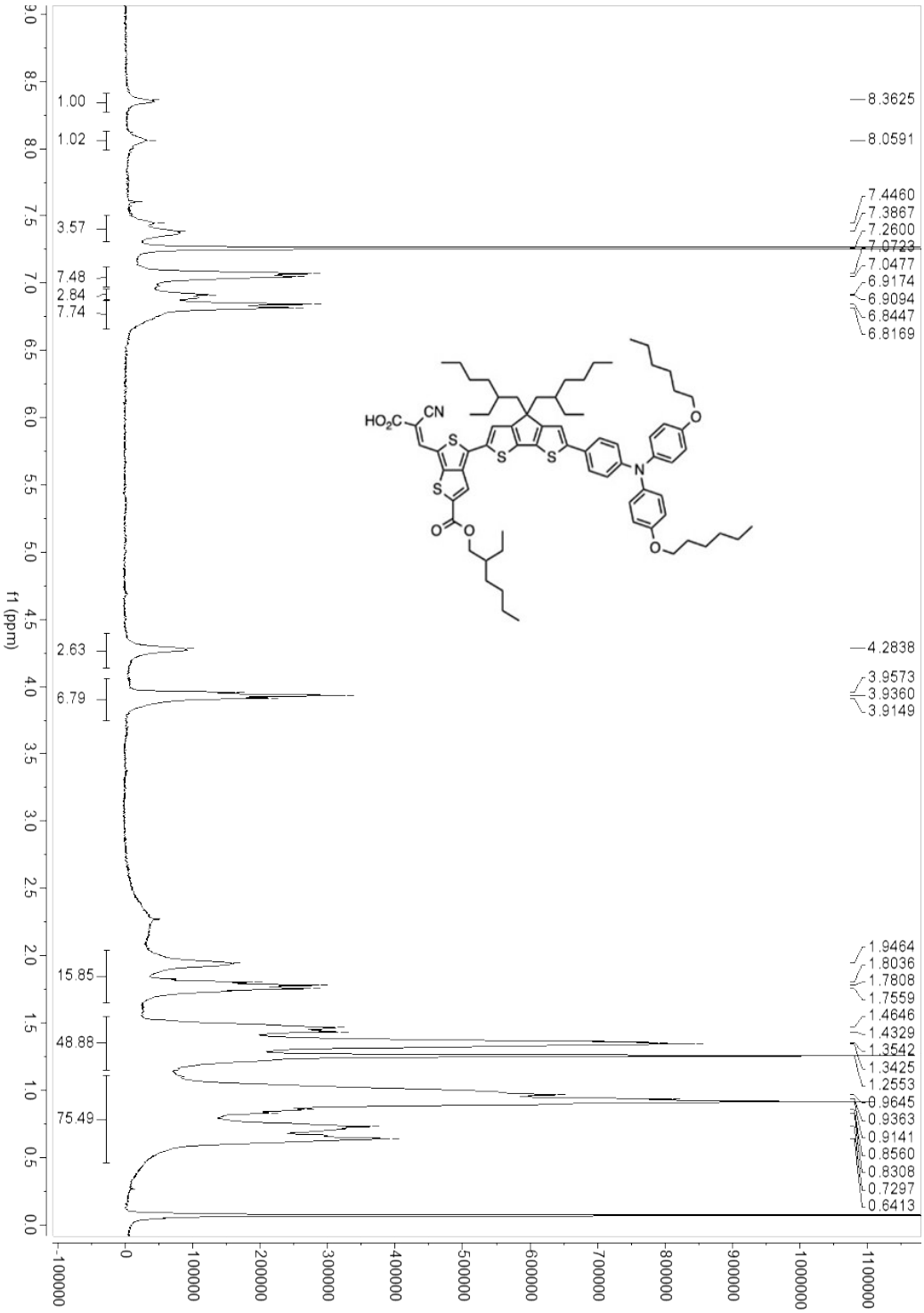

Figure S31. Compound **6** (b): ^{1}H NMR ($CDCl_3$), 300 MHz
Upon rigorous removal of residual solvents, peak resolution decreases due to aggregation of the final dye. Figure S30 shows a ^{1}H NMR with residual diethyl ether present, and Figure S31 shows after rigorous drying.

12. AP25 XYZ Coordinates from DFT Geometry Optimization

H	-4.152261	-2.628856	-0.582229
H	-6.548043	-2.176428	-0.650399
C	-6.379025	-0.121894	-0.012179
C	-5.459657	0.874472	0.365669
C	-4.10146	0.609132	0.409853
C	-3.584858	-0.657968	0.08764
C	-4.509988	-1.649383	-0.286192
C	-5.869474	-1.39384	-0.336785
H	-3.428937	1.395509	0.734799
H	-5.820278	1.857636	0.638525
C	5.650522	-0.699536	-0.00087
C	-10.628922	-2.930411	0.429891
C	-10.696115	-2.074113	-0.671748
C	-9.736867	-1.075289	-0.835615
C	-8.713834	-0.89903	0.095414
C	-8.663927	-1.753927	1.206731
C	-9.600581	-2.761444	1.366525
H	-11.477127	-2.177403	-1.412797
H	-9.790998	-0.420392	-1.69705
C	1.029049	-4.156015	-0.56298
H	-7.881222	-1.623636	1.944713
H	-9.568248	-3.425313	2.221905
C	-9.191564	2.046607	0.507695
C	-8.232251	1.468414	-0.322704
C	-7.768112	2.201864	-1.424852
C	-8.241917	3.478827	-1.673849
C	-9.209799	4.052673	-0.838797
C	-9.688699	3.324593	0.253147
H	-9.561641	1.489524	1.360185
C	3.614657	-2.176656	0.318849
H	-7.028154	1.763354	-2.083777
H	-7.887906	4.051979	-2.522112
C	5.993753	1.83739	0.477168
H	-10.435398	3.739536	0.916464
S	-0.968345	0.331703	-0.138062
C	6.361159	0.504518	0.117795
H	0.139019	-4.781125	-0.450887
C	4.247057	-0.957662	0.084047

O	5.871589	4.574019	1.153876
C	9.446281	-1.611451	-0.40975
C	10.68279	-1.132495	-0.760619
H	9.425964	-2.677234	-0.207132
S	6.763341	-2.000849	-0.311142
S	3.048756	0.326459	-0.169432
N	-7.7544	0.146034	-0.068555
C	-12.564584	-4.167561	-0.235192
H	-13.125667	-5.013201	0.158795
H	-13.225915	-3.296607	-0.305734
H	-12.186276	-4.417978	-1.232656
C	-10.586707	5.949884	-0.361982
H	-10.752174	6.927941	-0.8105
H	-11.531124	5.394136	-0.3491
H	-10.227422	6.079411	0.665103
O	-11.50409	-3.944155	0.683416
O	-9.615249	5.309139	-1.176752
C	10.913104	0.173671	-1.270621
C	7.111198	4.080973	0.947965
O	11.600297	-3.2652	-0.283771
O	8.124335	4.731463	1.050727
C	1.043653	-3.042299	0.505821
C	11.877392	-2.007898	-0.727208
N	11.085756	1.219168	-1.733981
O	12.989253	-1.671138	-1.051404
C	-2.156656	-0.949853	0.134782
C	-1.53033	-2.164354	0.356753
H	-2.087223	-3.06734	0.569013
C	-0.124662	-2.075523	0.321071
C	0.329961	-0.791008	0.072268
C	2.218507	-2.086554	0.304206
C	1.761347	-0.795922	0.059926
C	1.050655	-3.653099	1.923722
H	0.162302	-4.271448	2.078201
H	1.931092	-4.285821	2.065459
H	1.061884	-2.872082	2.686458
H	1.027089	-3.73354	-1.569692
H	1.907966	-4.798463	-0.460927
S	8.61455	1.858688	0.237168
H	4.173561	-3.083414	0.512948

C	7.774763	0.35515	-0.051314
C	8.194086	-0.957005	-0.278957
C	7.076938	2.653763	0.58672
H	4.989277	2.182996	0.667855
H	12.440276	-3.744217	-0.316749
C	5.814927	5.965999	1.51652
H	4.757721	6.189945	1.638454
H	6.355931	6.139929	2.447798
H	6.251675	6.582674	0.729799

13. PB1 XYZ Coordinates from DFT Geometry Optimization

C	0.384452	-0.502861	0.004987
C	-0.411456	-1.481608	-0.61998
C	-6.468091	-2.597925	-1.227154
C	-5.667805	-1.477831	-1.079352
C	-6.273624	-3.721802	-0.413376
C	-5.270351	-3.696763	0.559624
C	3.897177	2.467758	-0.262183
C	2.675579	1.877275	-0.17162
C	-4.660439	-1.443091	-0.105413
H	1.754128	2.434696	-0.243298
C	2.774499	0.459255	-0.014245
C	1.83581	-0.576841	-0.007262
O	-7.106138	-4.77349	-0.646375
C	4.133752	0.006939	0.012697
C	4.273985	-1.381896	0.01803
C	-6.963758	-5.942581	0.149322
C	-6.32118	5.700564	-0.077026
H	-5.284824	6.042719	0.020794
C	-4.519662	0.981373	0.215762
H	-6.991932	6.480621	0.278569
H	-6.53733	5.490206	-1.130351
C	3.310538	6.06071	-0.67962
H	2.31926	6.508126	-0.691593
H	3.906084	6.465261	0.139933
H	3.828374	6.246381	-1.621777
S	2.657385	-2.102267	0.009829
S	5.253024	1.339008	-0.142146
O	5.329665	4.33877	-0.543155
C	5.365258	-2.289239	-0.040561
C	6.688649	-2.128226	0.277275

H	5.111108	-3.285123	-0.388222
O	3.091478	4.650197	-0.494447
C	4.210269	3.89475	-0.444928
N	-3.85205	-0.273836	0.055573
O	7.114551	-4.305665	-0.556741
C	7.669977	-3.211417	0.032683
N	7.621829	-0.078789	1.530447
O	8.841465	-3.157481	0.31387
H	7.835524	-4.943344	-0.655034
C	7.212088	-0.986358	0.942416
O	-6.575406	4.567865	0.743068
C	-1.791846	-1.411887	-0.608234
C	-2.457837	-0.351988	0.041532
C	-1.666853	0.625567	0.679257
C	-0.286376	0.549005	0.657878
H	0.065014	-2.292332	-1.160195
H	-2.368798	-2.170179	-1.120575
H	-2.147368	1.435842	1.211393
H	0.285435	1.290764	1.201685
C	-4.481555	-2.557343	0.714057
H	-5.821452	-0.615818	-1.717335
H	-7.249533	-2.633329	-1.97629
H	-5.102296	-4.544129	1.210267
H	-3.714627	-2.539321	1.479434
C	-5.499101	1.140154	1.20567
C	-6.168814	2.343536	1.349291
C	-5.866742	3.428077	0.515232
C	-4.888325	3.280092	-0.471977
C	-4.232572	2.058741	-0.621844
H	-5.735356	0.308847	1.859098
H	-6.928153	2.474728	2.110429
H	-4.638884	4.095296	-1.137551
H	-3.485536	1.94633	-1.39884
H	-7.718427	-6.639707	-0.21035
H	-5.971209	-6.391118	0.030011
H	-7.142957	-5.73131	1.209363

14. References

[1] a) N. M. Shavaleev, R. Scopelliti, M. Grätzel, M. K. Nazeeruddin, *Inorganica Chim. Acta* **2013**, *404*, 210-214; b) S. Feldt, E. A. Gibson, E. Gabrielsson, S. Sun, G. Boschloo, A. Hagfeldt, *J. Am. Chem. Soc.* **2010**, *132*, 16714-16724.

[2] P. Brogdon, F. Giordano, G. A. Puneky, A. Dass, S. M. Zakeeruddin, M. K. Nazeeruddin, M. Gratzel, G. S. Tschumper, J. H. Delcamp, *Chem.: Eur. J.* **2016**, *22*, 694-703.

[3] R. Li, J. Liu, N. Cai, M. Zhang, P. Wang, *J. Phys. Chem. B* **2010**, *114*, 4461-4464.

[4] a) M. K. Nazeeruddin, S. M. Zakeeruddin, R. Humphry-Baker, M. Jirousek, P. Liska, N. Vlachopoulos, V. Shklover, C.-H. Fischer, M. Grätzel, *Inorg. Chem.* **1999**, *38*, 6298-6305; b) Y. Sun, A. C. Onicha, M. Myahkostupov, F. N. Castellano, *ACS Appl. Mater. Interfaces* **2010**, *2*, 2039-2045; c) Péchy, T. Renouard, S. M. Zakeeruddin, R. Humphry-Baker, P. Comte, P. Liska, L. Cevey, E. Costa, V. Shklover, L. Spiccia, G. B. Deacon, C. A. Bignozzi, M. Grätzel, *J. Am. Chem. Soc.* **2001**, *123*, 1613-1624. D) Y. Lee, S.-R. Jang, R. Vittal, K.-J. Kim, *New J. Chem.* **2007**, *31*, 2120-2126.

[5] M. J. Frisch, G. W. Trucks, H. B. Schlegel, G. E. Scuseria, M. A. Robb, J. R. Cheeseman, G. Scalmani, V. Barone, B. Mennucci, G. A. Petersson, H. Nakatsuji, M. Caricato, X. Li, H. P. Hratchian, A. F. Izmaylov, J. Bloino, G. Zheng, J. L. Sonnenberg, M. Hada, M. Ehara, K. Toyota, R. Fukuda, J. Hasegawa, M. Ishida, T. Nakajima, Y. Honda, O. Kitao, H. Nakai, T. Vreven, J. A. Montgomery Jr., J. E. Peralta, F. Ogliaro, M. J. Bearpark, J. Heyd, E. N. Brothers, K. N. Kudin, V. N. Staroverov, R. Kobayashi, J. Normand, K. Raghavachari, A. P. Rendell, J. C. Burant, S. S. Iyengar, J. Tomasi, M. Cossi, N. Rega, N. J. Millam, M. Klene, J. E. Knox, J. B. Cross, V. Bakken, C. Adamo, J. Jaramillo, R. Gomperts, R. E. Stratmann, O. Yazyev, A. J. Austin, R. Cammi, C. Pomelli, J. W. Ochterski, R. L. Martin, K. Morokuma, V. G. Zakrzewski, G. A. Voth, P. Salvador, J. J. Dannenberg, S. Dapprich, A. D. Daniels, Ö. Farkas, J. B. Foresman, J. V. Ortiz, J. Cioslowski, D. J. Fox, Gaussian, Inc., Wallingford, CT, USA, **2009**.

[6] a) M. Pazoki, U. B. Cappel, E. M. Johansson, A. Hagfeldt, G. Boschloo, *Energy Environ. Sci.* **2017**, 10, 672-709; b) M. Adachi, M. Sakamoto, J. Jiu, Y. Ogata, S. Isoda, *J. Phys. Chem. B* **2006**, *110*, 13872-13880; c) J. Nissfolk, K. Fredin, A. Hagfeldt, G. Boschloo, *J. Phys. Chem. B* **2006**, *110*, 17715-17718.

[7] X. Kang, J. Zhang, A. J. Rojas, D. O'Neil, P. Szymanski, S. R. Marder, M. A. El-Sayed, *J. Mater. Chem. A* **2014**, *2*, 11229-11234.

[8] G. Boschloo, L. Häggman, A. Hagfeldt, *J. Phys. Chem. B* **2006**, *110*, 13144-13150.

[9] X. Jiang, T. Marinado, E. Gabrielsson, D. P. Hagberg, L. Sun, A. Hagfeldt, *J. Phys. Chem. C* **2010**, *114*, 2799-2805.

[10] N. R. Neale, N. Kopidakis, d. L. van, M. Grätzel, A. J. Frank, *J. Phys. Chem. B* **2005**, *109*, 23183-23189.

[11] a) A. K. Chandiran, S. M. Zakeeruddin, R. Humphry-Baker, M. K. Nazeeruddin, M. Grätzel, F. Sauvage, *ChemPhysChem* **2017**, *18*, 2724-2731; b) A. Peddapuram, H. Cheema, R. E. Adams, R. H. Schmehl, J. H. Delcamp, *J. Phys. Chem. C* **2017**, *121*, 8770-8780.

[12] J. R. Jennings, Q. Wang, *J. Phys. Chem. C* **2010**, *114*, 1715-1724.

[13] D. Joly, L. Pelleja, S. Narbey, F. Oswald, J. Chiron, J. N. Clifford, E. Palomares, R. Demadrille, *Sci. Rep.* **2014**, *4*, 4033.

[14] a) T. Yamaguchi, T. Miyabe, T. Ono, H. Arakawa, *Chem.Comm.* **2010**, *46*, 5802-5804; b) H. Cheema, A. Islam, L. Han, B. Gautam, R. Younts, K. Gundogdu, A. El-Shafei, *J. Mater. Chem. A* **2014**, *34*, 14228-14235; c) T. Kinoshita, J. T. Dy, S. Uchida, T. Kubo, H. Segawa, *Nat. Photon.* **2013**, *7*, 535-539; d) T. Kinoshita, K. Nonomura, N. Joong Jeon, F. Giordano, A. Abate, S. Uchida, T. Kubo, S. I. Seok, M. K. Nazeeruddin, A. Hagfeldt, M. Gratzel, H. Segawa, *Nat. Commun.* **2015**, *6*, 8834; e) K.-L. Wu, S.-T. Ho, C.-C. Chou, Y.-C. Chang, H.-A. Pan, Y. Chi, P.-T. Chou, *Angew. Chem. Int. Ed.* **2012**, *51*, 5642-5646; f) N. V. Krishna, J. V. S. Krishna, S. P. Singh, L. Giribabu, L. Han, I. Bedja, R. K. Gupta, A. Islam, *J. Phys. Chem. C* **2017**, *121*, 6464-6477; g) L. Zhang, X. Yang, W. Wang, G. G. Gurzadyan, J. Li, X. Li, J. An, Z. Yu, H. Wang, B. Cai, *ACS Energy Lett.* **2019**, *4*, 943-951.

[15] H. Cheema, R. R. Rodrigues, J. H. Delcamp, *Energy Environ. Sci.* **2017**, *10*, 1764-1769.

[16] a) D. P. Hagberg, X. Jiang, E. Gabrielsson, M. Linder, T. Marinado, T. Brinck, A. Hagfeldt, L. Sun, *J. Mater. Chem.* **2009**, *19*, 7232-7238; b) N. Koumura, Z.-S. Wang, S. Mori, M. Miyashita, E. Suzuki, K. Hara, *J. Am. Chem. Soc.* **2006**, *128*, 14256-14257.